

**Design of RC Elements Subjected to In-plane Loading**

Késio Palácio, Paulo B. Lourenço, Joaquim A. O. Barros

Report 03-DEC/E-30

*The present research has been carried out under  
"Onderzoek protocol 8857"  
Ministry of Transport, Public Works and Water Management  
The Netherlands*

Date: December 2003

No. of Pages: 45

Keywords: reinforcement design, reinforced concrete, membrane elements



Escola de  
Engenharia



Departamento de  
Engenharia Civil



Universidade  
do Minho



## Contents

<b>1 Introduction</b> .....	<b>3</b>
<b>2 Yield Conditions for Membrane Elements</b> .....	<b>5</b>
2.1 Reinforcement Design Equations .....	7
<b>3 Cracked Membrane Model</b> .....	<b>12</b>
3.1 General Considerations .....	12
3.1.1 <i>Compatibility Conditions</i> .....	14
3.1.2 <i>Constitutive Laws</i> .....	16
3.2 Design Equations .....	17
<b>4 Numerical Implementation</b> .....	<b>27</b>
4.1 Numerical Routines .....	28
<b>5 Application Examples</b> .....	<b>33</b>
5.1 Deep Beam With One Opening .....	33
5.2 Deep Beam With Two Openings .....	39
<b>6 Conclusions</b> .....	<b>44</b>
<b>7 References</b> .....	<b>45</b>

# 1 Introduction

Reinforced concrete (RC) plane surface structures subjected to in-plane forces have many applications in the civil construction field, from foundation to roof structural elements. Shear walls, load-bearing walls and deep beams are some examples of these structures, see Figure 1.1.

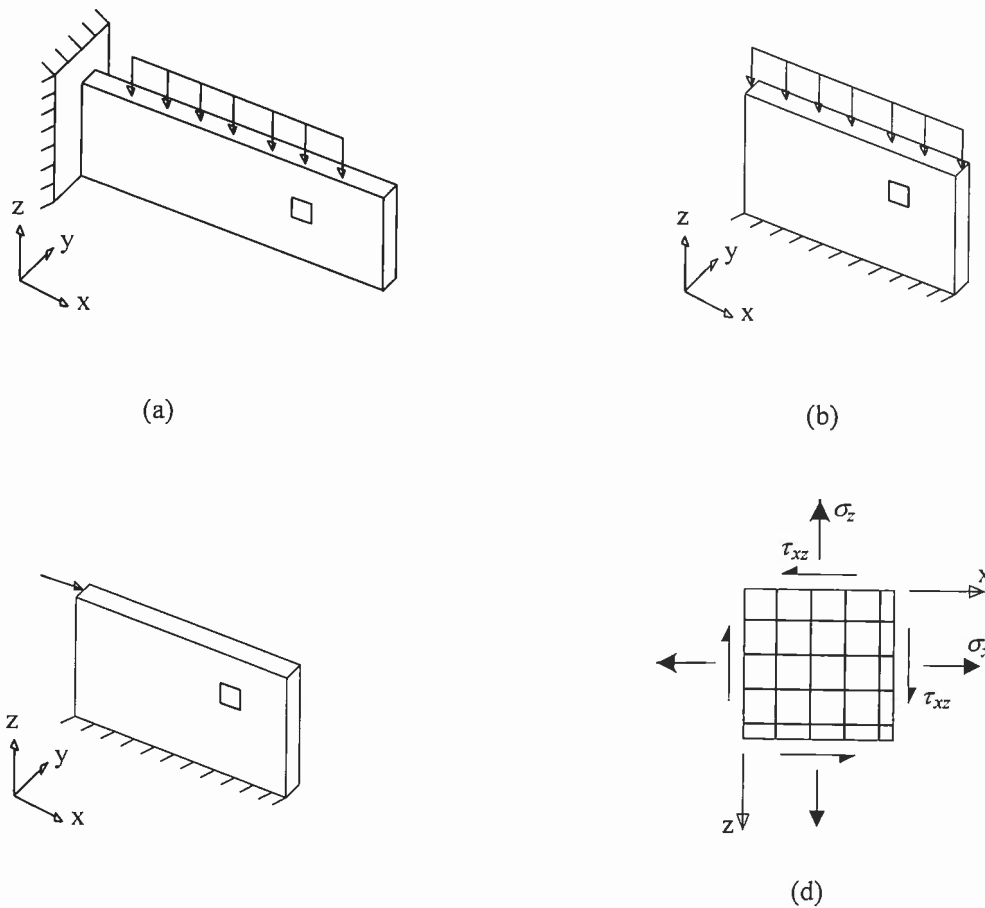


Figure 1.1 – Structural elements subjected to in-plane forces: a) deep beam; b) load-bearing wall; c) shear wall; d) general case of plane stress state

Structures of the type show in Figure 1.1 carry load primarily through the action of in-plane stresses. To determine the behavior of such structures, the response of a two-dimensional rectangular reinforced concrete element subject to plane stresses is considered. In



structural mechanics this element is usually denoted as *plate in plane stress* or *membrane*, which is used in finite element method (FEM) to model plane surface structures subjected to in-plane loadings. Thus, the distribution of stresses in these structures, before crack initiation, can be found by using a linear elastic finite-element analysis.

The use of linear elastic analysis techniques, such as FEM, has basically solved the first part of the design process of reinforced structural elements in plane stress, which is structural analysis. Now with relation to design itself, the solution is a complex task because of the number of unknowns is larger than the number of available equations from statics. Due to this fact, several theoretical models for the design and analysis of RC membrane elements have been proposed by many researchers, as for example the *yield criteria for disks with orthogonal reinforcement*, Nielsen (1971), the *modified compression field theory* (MCFT) from Vecchio and Collins (1986) and the *cracked membrane model* (CMM) developed by Kaufmann and Marti (1998). The last model combines the basic concepts of MCFT with the tension cord model developed by Marti *et al* (1998).

From CMM, simple design equations for cracked, orthogonally RC membranes have been recently proposed by Kaufmann (2002). These equations express the ultimate load of membrane elements in terms of the reinforcement ratios, yield strength of steel and the cylinder compressive strength of concrete, but accounting for the compression softening of the concrete as a result of introducing the compatibility of deformation. In the present work, the design equations were implemented in a computer program and incorporated in the DIANA 8.1 finite-element package through its post-processing interface, extending the use of the finite-element package, from an analysis tool to a design tool for RC membrane elements.

The presentation of the yield conditions for membrane elements, as well as the correspondent design equations according to the yield criteria proposed by Nielsen (1971), is given in Chapter 2. In the following chapter the failure surfaces of CMM in relation to limit analysis is introduced, yielding the design expressions for cracked, orthogonally RC membrane elements. In Chapter 4 the numerical procedure that was developed to implement the design equations is presented. Chapter 5 shows two application examples, with comparisons between the novel formulation and the traditional design equations according to the yield criteria of Nielsen (1971). Finally, Chapter 6 presents the conclusions of the present work.

## 2 Yield Conditions for Membrane Elements

It is straightforward to correlate the state of stress of framed structures with its maximum stress (strength) because they are both uniaxial. However, when dealing with a general or plane stress state, how can one correlate such stress state to a single component, whose material strength(s) is measured in uniaxial tests, in order to estimate yield or failure tendency? At present there is no fundamental rationale for such a correlation, and a failure theory is needed to develop failure criteria (or yield conditions) for structural elements whose stress state is not uniaxial. This is the case of membrane elements.

Yield conditions for membrane elements were firstly introduced by Nielsen (1964), for the case of isotropic reinforcement. This same author extended this concept to orthogonal reinforcement, Nielsen (1971), considering in both cases the response of concrete in compression as perfectly plastic. Only a brief description will be given here and the reader is referred to Nielsen (1971) or Kaufmann (1998) for a comprehensive review.

Consider an orthogonally reinforced membrane element subjected to in-plane shear  $\tau_{xz}$  and normal  $\sigma_x$ ,  $\sigma_z$  stresses, see Figure 2.1a. Firstly the yield surface for this element is built considering the stress contributions of reinforcement and plain concrete separately. Then the yield surface is obtained as the envelope of all linear combinations of admissible states of stress in the reinforcement and in the concrete, b. The surface obtained in such a way consists of seven different yield regimes; however, for design purposes, just the regimes identified in Figure 2.1c are usually relevant. These design regimes are described by the following yield criteria

$$\begin{aligned}\Phi_1 &= \tau_{xz}^2 - (\rho_x f_{yx} - \sigma_x) \cdot (\rho_z f_{yz} - \sigma_z) = 0 & (a) \\ \Phi_2 &= \tau_{xz}^2 - (f_c - \rho_z f_{yz} + \sigma_z) \cdot (\rho_x f_{yx} - \sigma_x) = 0 & (b) \\ \Phi_3 &= \tau_{xz}^2 - (f_c - \rho_x f_{yx} + \sigma_x) \cdot (\rho_z f_{yz} - \sigma_z) = 0 & (c) \\ \Phi_4 &= \tau_{xz}^2 - f_c^2/4 = 0 & (d)\end{aligned}\tag{2.1}$$

where  $\rho_x$ ,  $\rho_z$  are the reinforcement ratios in  $x$  and  $z$  directions, respectively, and  $f_{yx}$ ,  $f_{yz}$  their correspondent yield strengths;  $f_c$  is the effective concrete compressive strength, in order to take into account the perfectly plastic behavior assumed.

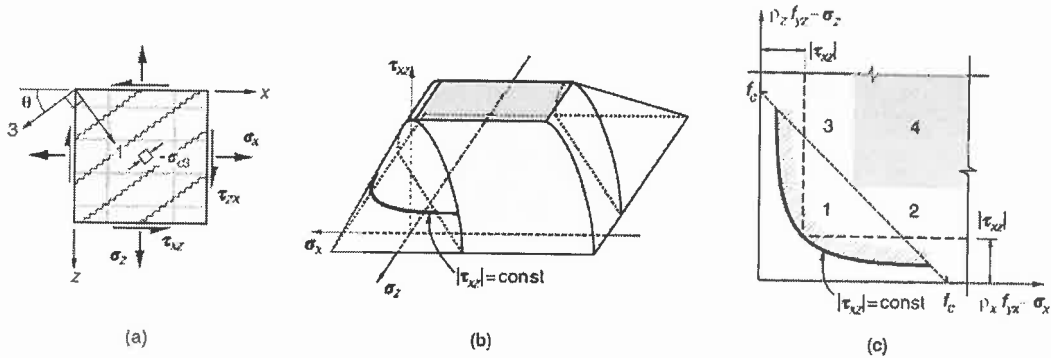


Figure 2.1- Limit analysis: a) applied stresses to orthogonally reinforced membrane b) yield surface for perfectly plastic behavior; c) yield regimes for reinforcement design

Each point on the yield surface corresponds to a potential failure stress combination. According to the associated flow rule

$$\dot{\epsilon}_x = \dot{\lambda} \frac{\partial \Phi}{\partial \sigma_x} \quad \dot{\epsilon}_z = \dot{\lambda} \frac{\partial \Phi}{\partial \sigma_z} \quad \dot{\gamma}_{xz} = \dot{\lambda} \frac{\partial \Phi}{\partial \tau_{xz}} \quad (2.2)$$

the plastic strain rates  $\dot{\epsilon}_x$ ,  $\dot{\epsilon}_z$ , and  $\dot{\gamma}_{xz}$  are proportional to the components of the outward normal to the yield surface in the stress point under consideration; the symbol  $\dot{\lambda}$  denotes an arbitrary non-negative factor. For stress points satisfying more than one of the criteria, equation (2.1), the flow rule, equation (2.2), has to be applied separately for each regime and the associated strain rates must be superimposed. Knowing the strain rates, associated Mohr's circles can be drawn and the inclination  $\theta$  of the minimum principal compressive direction  $\sigma_{c3}$  to the  $x$ -axis can be determined from

$$\cot 2\theta = \frac{\dot{\epsilon}_z - \dot{\epsilon}_x}{\dot{\gamma}_{xz}} \quad \text{or} \quad \cot \theta = \frac{\dot{\epsilon}_z - \dot{\epsilon}_x}{\dot{\gamma}_{xz}} + \sqrt{\left(\frac{\dot{\epsilon}_z - \dot{\epsilon}_x}{\dot{\gamma}_{xz}}\right)^2 + 1} \quad (2.3)$$

which yields the following expressions for the design regimes studied:

$$\Phi_1 : \cot^2 \theta = \frac{(\rho_x f_{yx} - \sigma_x)}{(\rho_z f_{yz} - \sigma_z)} \quad (a)$$



$$\Phi_2 : \cot^2 \theta = \frac{(f_c - \rho_z f_{yz} + \sigma_z)}{(\rho_z f_{yz} - \sigma_z)} \quad (b)$$

$$\Phi_3 : \cot^2 \theta = \frac{(f_c - \rho_x f_{yx} + \sigma_x)}{(\rho_x f_{yx} - \sigma_x)} \quad (c) \quad (2.4)$$

$$\Phi_4 : \cot^2 \theta = 1 \quad (d)$$

Regime 1 corresponds to under-reinforced membrane elements where failure is governed by yielding of both reinforcements. In Regimes 2 and 3 concrete crushes and one of the reinforcements yields. For Regime 4 concrete also crushes but both reinforcements remain elastic. In other words, it means that, if  $f_c \geq \sigma_{c3}$  is not satisfied, being  $\sigma_{c3}$  the minimum principal concrete compressive stress, three situations are possible to happen:

- i) concrete crushes and the  $x$ -reinforcement remain elastic whereas  $z$ -reinforcement, which is weaker, yields (Regime 2);
- ii) concrete crushes and the  $z$ -reinforcement remain elastic whereas  $x$ -reinforcement, which is weaker, yields (Regime 3);
- iii) concrete crushes and both reinforcements remain elastic (Regime 4).

## 2.1 Reinforcement Design Equations

This section addresses the reinforcement design equations for Regime 1, as given in Nielsen (1971). It is stressed that the design cases explored by the author are restricted only to Regime 1, whose behavior, as stated before, is based on yielding of both orthogonal reinforcements without crushing of concrete.

From equations (2.1a) and (2.4a) it is possible to obtain

$$\rho_x f_{yx} = \sigma_x + \tau_{xz} \cot \theta \quad (a)$$

$$\rho_z f_{yz} = \sigma_z + \tau_{xz} \tan \theta \quad (b) \quad (2.5)$$

As indicated in Figure 2.1c, equation (2.5) provides a parametric representation of lines of equal shear stress  $\tau_{xz}$ . As equation (2.5) is only valid in Regime 1, the condition of no-

crushing of concrete must be satisfied,  $f_c \geq \sigma_{c3}$ . The value of  $\sigma_{c3}$  can be obtained from equilibrium conditions, see Figure 2.2, and it is equal to

$$-\sigma_{c3} = \tau_{xz} \cdot \left( \cot \theta + \frac{1}{\cot \theta} \right) \quad (2.6)$$

Substituting the root of equation (2.4a) into equation (2.6),

$$-\sigma_{c3} = \rho_x f_{yx} + \rho_z f_{yz} - \sigma_x - \sigma_z \quad (2.7)$$

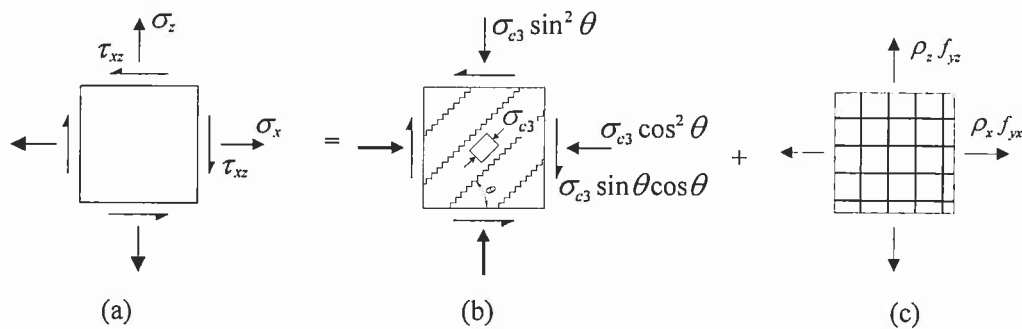


Figure 2.2 – External and internal stresses on membrane element: a) applied stresses; b) concrete stresses; c) steel stresses

The total reinforcement area can be obtained from equations (2.5a) and (2.5b), being equal to

$$\rho_x f_{yx} + \rho_z f_{yz} = \sigma_x + \sigma_z + \tau_{xz} (\tan \theta + \cot \theta) \quad (2.8)$$

As the last term of equation (2.8) must be positive,  $\tau_{xz}$  and  $\theta$  must have the same sign. Therefore, the minimum value of total reinforcement corresponds to  $\theta = \pm \pi/4$ . For these values of  $\theta$ , having  $\rho_x f_{yx} \geq 0$  and  $\rho_z f_{yz} \geq 0$ , equations (2.5a) yields  $\sigma_x \geq -|\tau_{xz}|$  and equation (2.5b),  $\sigma_z \geq -|\tau_{xz}|$ . Otherwise the value of  $\theta$  has to be changed. Therefore four different cases have to be considered.





- Case 1 -  $A_{sx} \neq 0$  and  $A_{sz} \neq 0$

$$\begin{aligned}\sigma_x &\geq -|\tau_{xz}| & \sigma_z &\geq -|\tau_{xz}| \\ \rho_x f_{yx} &= \sigma_x + |\tau_{xz}| & \rho_z f_{yz} &= \sigma_z + |\tau_{xz}| \\ \theta &= \pm \frac{\pi}{4} & -\sigma_{c3} &= \rho_x f_{yx} + \rho_z f_{yz} - \sigma_x - \sigma_z\end{aligned}$$

- Case 2 -  $A_{sx} = 0$  and  $A_{sz} \neq 0$

$$\begin{aligned}\sigma_x < -|\tau_{xz}| &\Rightarrow \rho_x f_{yx} = 0 \\ \text{From Equation (2.5a): } \tan \theta &= -\frac{\sigma_x}{\tau_{xz}} \\ \text{From Equation (2.5b): } \rho_z f_{yz} &= \sigma_z - \frac{\tau_{xz}^2}{\sigma_x} \\ \rho_z f_{yz} \geq 0 &\Rightarrow \sigma_z \geq \frac{\tau_{xz}^2}{\sigma_x} & -\sigma_{c3} &= \rho_z f_{yz} - \sigma_x - \sigma_z\end{aligned}$$

- Case 3 -  $A_{sx} \neq 0$  and  $A_{sz} = 0$

$$\begin{aligned}\sigma_z < -|\tau_{xz}| &\Rightarrow \rho_z f_{yz} = 0 \\ \text{From Equation (2.6b): } \tan \theta &= -\frac{\tau_{xz}}{\sigma_z} \\ \text{From Equation (2.5b): } \rho_x f_{yx} &= \sigma_x - \frac{\tau_{xz}^2}{\sigma_z} \\ \rho_x f_{yx} \geq 0 &\Rightarrow \sigma_x \geq \frac{\tau_{xz}^2}{\sigma_z} & -\sigma_{c3} &= \rho_x f_{yx} - \sigma_x - \sigma_z\end{aligned}$$

- Case 4 -  $A_{sx} = 0$  and  $A_{sz} = 0$  (biaxial compression)

$$\left\{ \begin{array}{l} \sigma_x < -|\tau_{xz}| \\ \sigma_z < \frac{\tau_{xz}^2}{\sigma_x} \end{array} \right. \quad \text{or} \quad \left\{ \begin{array}{l} \sigma_z < -|\tau_{xz}| \\ \sigma_x < \frac{\tau_{xz}^2}{\sigma_z} \end{array} \right. \Rightarrow \left\{ \begin{array}{l} \rho_x f_{yx} = 0 \\ \rho_z f_{yz} = 0 \\ \sigma_{c1,3} = \frac{\sigma_x + \sigma_z}{2} \pm \sqrt{\left(\frac{\sigma_x - \sigma_z}{2}\right)^2 + \tau_{xz}^2} \end{array} \right.$$

These formulae correspond to the optimum direction of the concrete compression, i.e., the value of  $\theta$  leading to the minimum amount of reinforcement.

The reinforcement design, per unit of length, is then obtained from,

$$A_{sx} = \frac{\rho_x f_{yx}}{f_{ytx}} h \quad A_{sz} = \frac{\rho_x f_{yz}}{f_{ydz}} h \quad (2.9)$$

where  $h$  is the thickness of membrane element.

The value of  $f_c$ , which limits stress in concrete, can be given according to the recommendations of MC90, namely:

- Uncracked zones: Case 4

$$f_{cd1} = 0.85 \left[ 1 - \frac{f_{ck}}{250} \right] f_{cd} \quad (2.10)$$

$$f_c = K f_{cd1} \quad (2.11)$$

Where  $f_{ck}$  and  $f_{cd}$  are, respectively, the characteristic and the design cylinder compressive strength, expressed in MPa. The parameter  $K$  takes into account the confinement effect of concrete due to biaxial compression state and reads

$$K = \frac{1 + 3.65\alpha}{(1 + \alpha)^2}, \quad \text{with } \alpha = \frac{\sigma_{e3}}{\sigma_{c1}}$$



- Cracked zones: Cases 1 - 3

At cracked zones, the compressive strength of concrete may be reduced by the effect of transverse tension from reinforcement and by the need to transmit force across the cracks,

$$f_c = 0.60 \left[ 1 - \frac{f_{ck}}{250} \right] f_{cd} \quad (2.12)$$

The numerical implementation and discussions of practical use of these design equations can be found in Lourenço and Figueiras (1993, 1995).

### 3 Cracked Membrane Model

The cracked membrane model (CMM) of Kaufmann and Marti (1998) is a new model for the cracked, orthogonally reinforced concrete panels subjected to a plane stress state, which further extends the formulation of Chapter 2 taking into account the deformation compatibility. It combines the basic concepts of the compression field approaches, which is described in Section 3.1, with a recently developed tension chord model of Marti *et al* (1998). This chapter summarizes the basic concepts of the main numerical issues of the CMM.

#### 3.1 General Considerations

Some fundamental aspects of the behavior of CMM are given by using compression field approaches, which satisfy equilibrium and compatibility conditions. Consider an orthogonally RC membrane element, with a set of parallel, uniformly spaced cracks, see Figure 3.1. Equilibrium of the stresses at cracks requires, see Figure 3.1b,

$$\begin{aligned}\sigma_x &= \rho_x \sigma_{sx} + \sigma_{cn} \sin^2 \theta + \sigma_{cr} \cos^2 \theta - \tau_{cni} \sin(2\theta) \\ \sigma_z &= \rho_z \sigma_{sz} + \sigma_{cn} \cos^2 \theta + \sigma_{cr} \sin^2 \theta + \tau_{cni} \sin(2\theta) \\ \tau_{xz} &= (\sigma_{cn} - \sigma_{cr}) \sin \theta \cos \theta - \tau_{cni} \cos(2\theta)\end{aligned}\quad (3.1)$$

where  $n$  and  $t$  are the coordinates aligned with the crack direction;  $\sigma_{cn}$  and  $\sigma_{cr}$  are the concrete stress normal and parallel to the direction of cracking, respectively, and  $\tau_{cni}$  is the shear stress;  $\sigma_{sx}$  and  $\sigma_{sz}$  are the stresses in  $x$  and  $z$  reinforcements, respectively.

Considering steel and bond stresses being given by equivalent stresses resulting from a uniform distribution in transverse direction between the individual reinforcing bars, and assuming homogeneous material properties one can conclude that the displacements at the cracks as well as the strains in concrete between the cracks are independent of the coordinate  $t$ , see Figure 3.1c. Thus,

$$\varepsilon_n = \frac{\partial u_c}{\partial n} \quad \varepsilon_t = \frac{\partial v_c}{\partial t} \quad \gamma_{nt} = \frac{\partial u_c}{\partial t} + \frac{\partial v_c}{\partial n}\quad (3.2)$$

where  $u_c$  and  $v_c$  are the concrete displacements in  $n$  and  $t$  directions. As the displacement  $u_c$  is only a function of  $n$  and  $\partial\gamma_m/\partial t = 0$  leads to  $\partial\varepsilon_i/\partial n = 0$ , implying that  $\varepsilon_i$  must be constant.

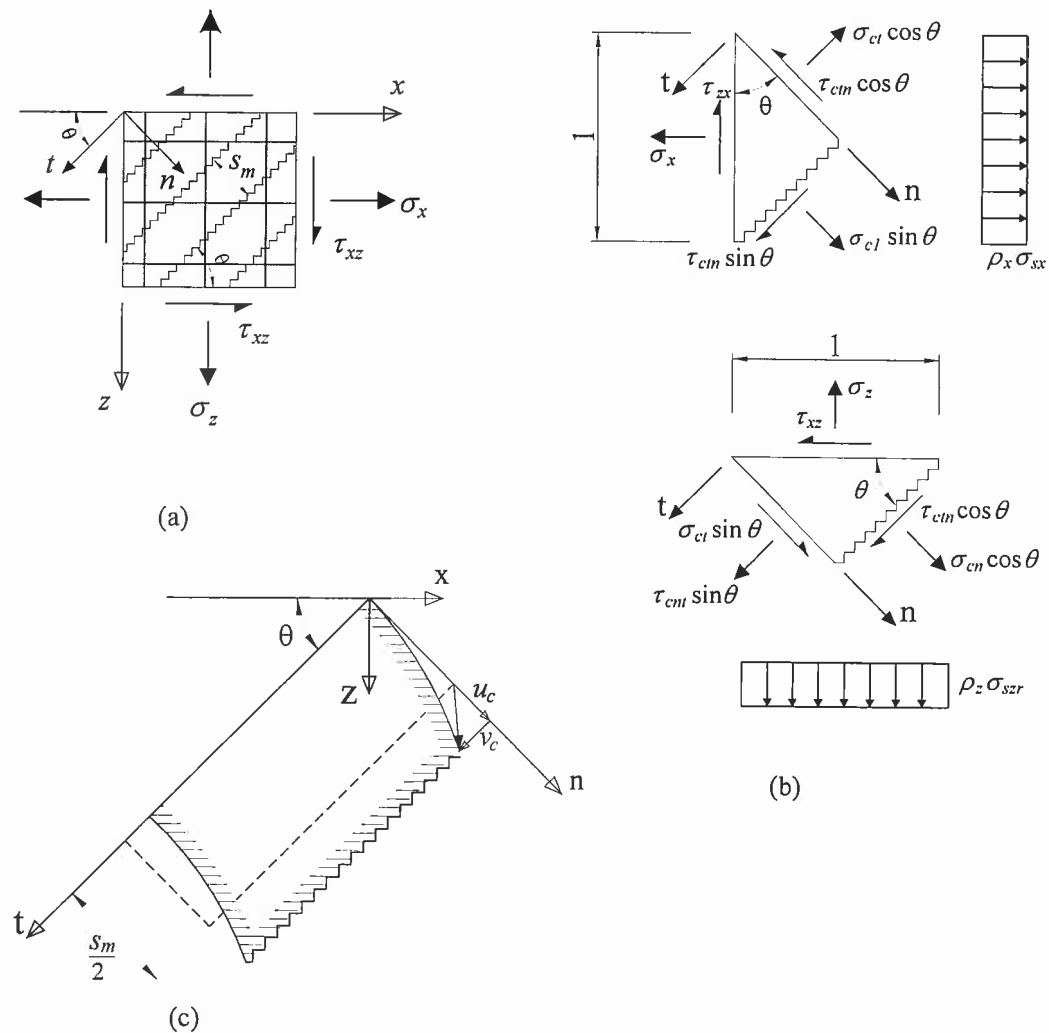


Figure 3.1 – Cracked membrane: a) notation; b) stresses at crack; c) displacements

The basic assumptions of the CMM are (i) crack faces are assumed to be stress free and able to rotate and (ii) the concrete principal stresses and principal strains are coincident. These assumptions lead to  $\sigma_{cn} = 0$  and  $\tau_{cni} = 0$ , meaning that equation (3.1) reduces to



$$\sigma_x = \rho_x \sigma_{sx} + \sigma_{c3} \cos^2 \theta \quad (a)$$

$$\sigma_z = \rho_z \sigma_{sz} + \sigma_{c3} \sin^2 \theta \quad (b) \quad (3.3)$$

$$\tau_{xz} = -\sigma_{c3} \sin \theta \cos \theta \quad (c)$$

where  $\sigma_{c3} = \sigma_{ct}$  and  $\sigma_{c1} = \sigma_{cn} = 0$ , given the fact that the  $n$  and  $t$  axes are coincident with the major and minor principal stress and strain axes of concrete, respectively.

### 3.1.1 Compatibility Conditions

Due to the fact that the cracked concrete is considered as a material with coinciding principal stresses and strains axes, which is the essence of the compression field approach, one can determine the state of strain and stress along any direction through the Mohr's circle. From the strain circle, see Figure 3.2a, the following strain relationships can be formulated:

$$\tan \theta = \frac{\varepsilon_x - \varepsilon_3}{\gamma_{xz}/2} \quad (3.4)$$

$$\cot \theta = \frac{\varepsilon_z - \varepsilon_3}{\gamma_{xz}/2} \quad (3.5)$$

$$\varepsilon_x + \varepsilon_z = \varepsilon_1 + \varepsilon_3 \quad (3.6)$$

where  $\varepsilon_x$ ,  $\varepsilon_z$  and  $\gamma_{xz}$  are the average total strains in the cracked membrane element, being  $x$  and  $z$  the orthogonal directions of the reinforcement, and being  $\varepsilon_1$  and  $\varepsilon_3$  the principal average strains.

Eliminating  $\gamma_{xz}$  in equations (3.4) and (3.5), one gets

$$\tan^2 \theta = \frac{\varepsilon_x - \varepsilon_3}{\varepsilon_z - \varepsilon_3} \quad \text{or} \quad \cot^2 \theta = \frac{\varepsilon_z - \varepsilon_3}{\varepsilon_x - \varepsilon_3} \quad (3.7)$$

Associating equations (3.7) and (3.6),

$$\varepsilon_1 = \varepsilon_x + (\varepsilon_x - \varepsilon_3) \cot^2 \theta \quad (3.8)$$

Similarly for stresses, the following relationships can be found with the aid of Mohr's circle, see Figure 3.2b:

$$\sigma_{cx} = \sigma_{c1} - \tau_{cxz} \cot \theta \quad (a)$$

$$\sigma_{cz} = \sigma_{c1} - \tau_{cxz} \tan \theta \quad (b) \quad (3.9)$$

$$\sigma_{c3} = \sigma_{c1} - \tau_{cxz} \left( \cot \theta + \frac{1}{\cot \theta} \right) \quad (c)$$

being  $\sigma_{cx}$ ,  $\sigma_{cz}$  and  $\tau_{cxz}$  the stress components of concrete, and being  $\sigma_{c1}$  and  $\sigma_{c3}$  its principal stresses.

Disregarding the tensile strength of concrete,  $\sigma_{c1} = 0$ , and considering the applied shear stress being resisted only by concrete, i.e.  $\tau_{cxz} = \tau_{xz}$ , the compressive principal stress of the concrete, equation (3.3c), becomes:

$$\sigma_{c3} = -\tau_{xz} \left( \cot \theta + \frac{1}{\cot \theta} \right) \quad (3.10)$$

which is identical to equation (2.6).

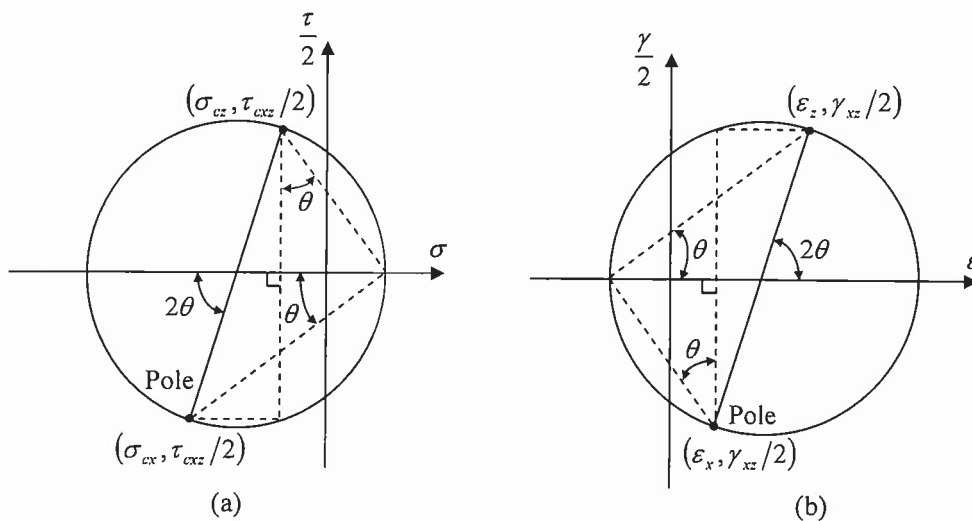


Figure 3.2 – Mohr's circle for: a) strains; b) concrete stresses

### 3.1.2 Constitutive Laws

Steel and bond shear stresses are treated according to Figure 3.3b, where the basic concepts of the tension chord model are extended to cracked membrane elements, see Figure 3.3c. As a result, both reinforcements are treated as tension chords.

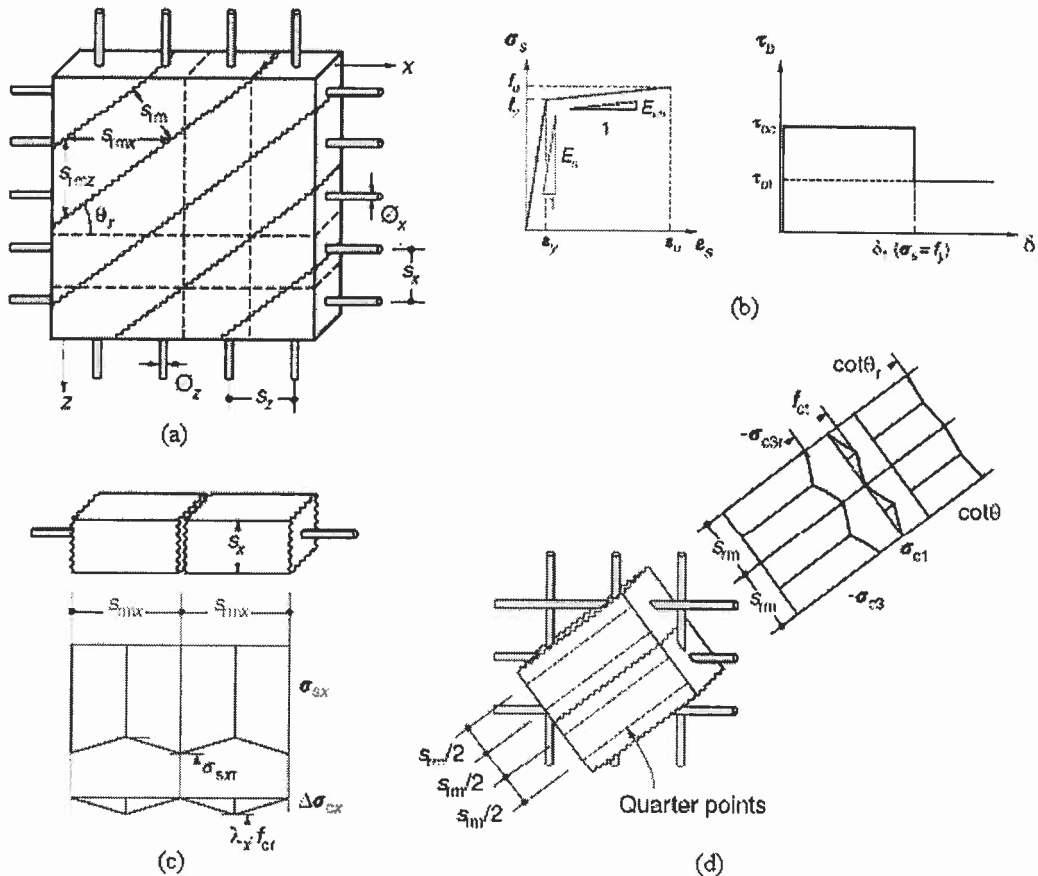


Figure 3.3 – Cracked membrane model: a) notation; b) steel constitutive relationships; c) steel stresses in  $x$ -direction ( $\Delta\sigma_{sx}$  = tension stiffening stress); d) concrete principal stresses.

For concrete, a parabolic stress-strain relationship is assumed for the principal compressive stress  $\sigma_{c3}$  at cracks, whereby compression softening is taken into account, see Kaufmann (1998), i.e.,



$$\sigma_{c3} = f_c (\varepsilon_3^2 + 2\varepsilon_3 \varepsilon_{co}) / \varepsilon_{co}^2 \quad (3.11)$$

and

$$f_c = \frac{(f_c')^{2/3}}{0.4 + 30\varepsilon_1} \leq f_c' \quad \text{in MPa} \quad (3.12)$$

where  $\varepsilon_{co}$  is the concrete strain at the peak compressive stress  $f_c$  and  $f_c'$  is the cylinder concrete compressive strength.

Thus, considering the average strains  $\varepsilon_x$ ,  $\varepsilon_z$ , and  $\varepsilon_3$  as the primary unknowns, all quantities in equation (3.3) can be expressed as functions of these three unknowns. In fact, the stresses  $\sigma_{sx}$  and  $\sigma_{sz}$  in reinforcements are derived from the constitutive equations of the tension chord model, and the stress in concrete  $\sigma_{c3}$ , from equations (3.11) and (3.12). Therefore, for a given set of applied stresses,  $\sigma_x$ ,  $\sigma_z$  and  $\tau_{xz}$ , the strains  $\varepsilon_x$ ,  $\varepsilon_z$ , and  $\varepsilon_3$  can be determined by means of an iterative numerical procedure.

### 3.2 Design Equations

By introducing the assumptions of limit analysis, Kaufmann (2002) obtained expressions to determine ultimate load of reinforced concrete panels in terms of the reinforcement ratios and the cylinder compressive strength of concrete ( $f_c'$ ). Therefore these expressions are suitable for design purposes. They were derived on the basis of the CMM with link to limit analysis.

Failure surfaces according to the general numerical method of the cracked membrane model can be generated by evaluating the peak shear stress for a certain range of reinforcement ratios,  $\rho_x$  and  $\rho_z$ , see Figure 3.4a. The failure surface obtained in this way is quite similar to the yield surface for perfectly plastic behavior (Figure 3.4b). In the latter case, which correspond to limit analysis, the surface was built using the yield criteria given in equation (2.1) and setting  $f_c = 1.7(f_c')^{2/3}$  (in MPa). In either case, the four regimes identified in Figure 3.4 have the same characteristics of those described in Chapter 2. Therefore, the results obtained from limit analysis and the cracked membrane model are quite similar.

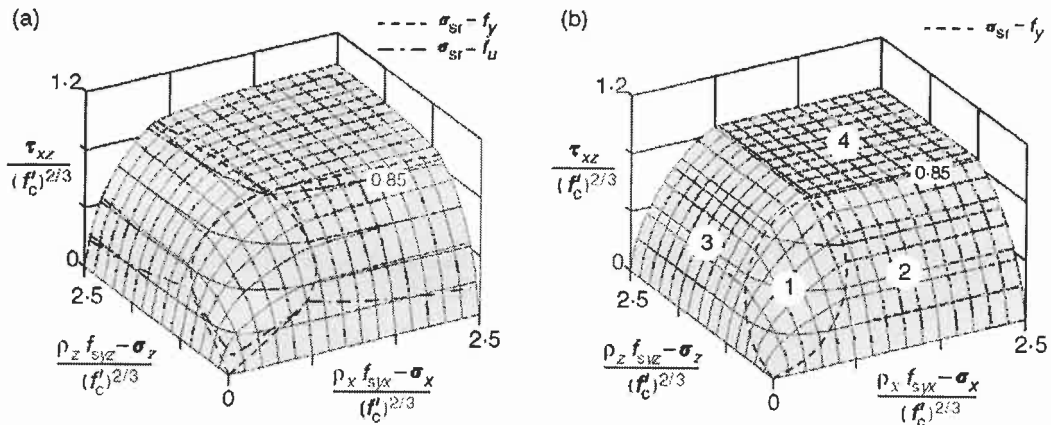


Figure 3.4- Failure surfaces: a) cracked membrane model; b) limit analysis, accounting for compression softening of the concrete [from Kaufmann (1998)]

Failure loads obtained from the cracked membrane model exceed those obtained from limit analysis in many situations, primarily because of strain-hardening of the reinforcement. However, failure loads can still be obtained from limit analysis by adopting a suitable value for the concrete compressive strength  $f_c$ , as for example the expression for  $f_c$  used in the cracked membrane model, equation (3.12). According to this expression,  $f_c$  depends on the principal tensile strain  $\varepsilon_1$ , which cannot be determined from limit analysis. However,  $\varepsilon_1$  can be expressed in terms of  $\rho_x f_{yx} - \sigma_x$  and  $\rho_x f_{yz} - \sigma_z$  if certain assumptions are made. Below the determination of  $\varepsilon_1$ , given by equation (3.8), and the correspondent expression of  $f_c$  for each Regime are described. Afterwards, the designs equations are finally provided.

#### a) Regime 1

Assuming a linear elastic-perfectly plastic stress-strain relationship for the reinforcement,  $\varepsilon_1$  can thus be determined along the boundary of Regimes 1 and 2 (see Figure 3.5), where the  $z$ -reinforcement yields (the weaker), the concrete crushes, and the  $x$ -reinforcement is at the onset of yielding.

The value of  $\cot^2 \theta$  in equation (3.8) for Regime 1 is given by equation (2.4a), which is  $\cot^2 \theta = (\rho_x f_{yx} - \sigma_x) / (\rho_z f_{yz} - \sigma_z)$ . The value of  $\varepsilon_3 = \varepsilon_{co} \cong 0.002$  is assumed since



concrete crushes and  $\varepsilon_x \approx 0.8 f_{yx} / E_s \cong 0.002$  (the value of 0.8 is adopted to take into account tension stiffening effects). Introducing these values into equation (3.6), one gets

$$\varepsilon_1 = 0.002 + 0.004 \cdot \frac{\rho_x f_{yx} - \sigma_x}{\rho_z f_{yz} - \sigma_z} \quad (3.13)$$

at the boundary of Regimes 1 and 2. Substituting this equation into the expression of  $f_c$ , equation (3.12), one gets

$$f_c^1 = \frac{(f_c')^{2/3}}{0.46 + 0.12 \cdot \frac{\rho_x f_{yx} - \sigma_x}{\rho_z f_{yz} - \sigma_z}} \quad (3.14)$$

for the boundary of Regimes 1 and 2. The principal concrete compressive stress in Regime 1 is equal to  $-\sigma_{c3} = \rho_x f_{yx} + \rho_z f_{yz} - \sigma_x - \sigma_z$ . Observing that  $\sigma_{c3}$  must not exceed  $f_c$ , one obtains

$$\frac{(f_c')^{2/3}}{\rho_x f_{yx} + \rho_z f_{yz} - \sigma_x - \sigma_z} \geq 0.46 + 0.12 \frac{\rho_x f_{yx} - \sigma_x}{\rho_z f_{yz} - \sigma_z} \quad (3.15)$$

for the boundary of Regimes 1 and 2, being the reinforcement in the  $x$ -direction stronger than the reinforcement in the  $z$ -direction,  $(\rho_x f_{yx} - \sigma_x) > (\rho_z f_{yz} - \sigma_z)$ . In the case of  $(\rho_z f_{yz} - \sigma_z) > (\rho_x f_{yx} - \sigma_x)$ , which corresponds to the boundary of Regimes 1 and 3, the condition of the principal concrete compressive stress  $\sigma_{c3}$  in Regime 1 not exceeding  $f_c$  is given by

$$\frac{(f_c')^{2/3}}{\rho_x f_{yx} + \rho_z f_{yz} - \sigma_x - \sigma_z} \geq 0.46 + 0.12 \frac{\rho_z f_{yz} - \sigma_z}{\rho_x f_{yx} - \sigma_x} \quad (3.16)$$

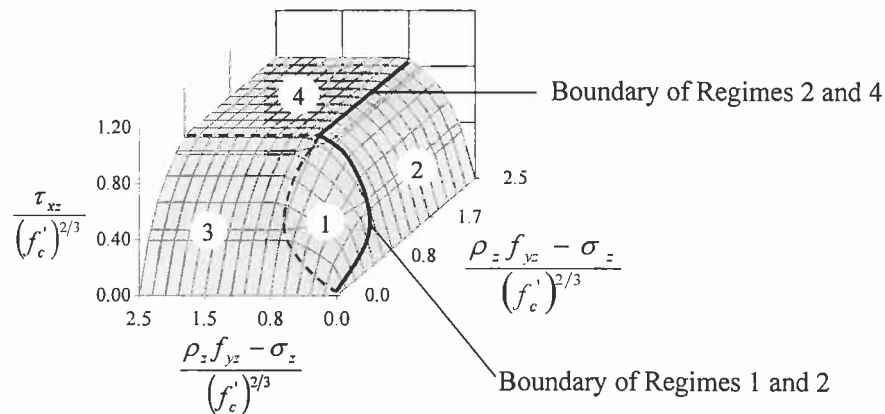


Figure 3.5– Representation of Boundary of Regimes

### b) Regimes 2, 3 and 4

In Regimes 2, 3 and 4, the failure load depends on  $f_c$  and thus on the principal tensile strain  $\varepsilon_1$ . For values of  $\rho_x f_{yx} - \sigma_x$  and  $\rho_x f_{yz} - \sigma_z$  higher than along the boundary to Regime 1, the steel stresses in the  $x$ -reinforcement (Regime 2) or in both reinforcements (Regime 4) are below the yield stress  $f_y$ . The strains ( $\varepsilon$ ) in the non-yielding reinforcements decrease for higher reinforcement ratios and hence,  $f_c$  increases. This effect is neglected here, assuming that the strains in the non-yielding reinforcements are equal to  $\varepsilon \approx 0.8 f_y / E_s \cong 0.002$  throughout Regimes 2, 3 and 4.

#### b.1) Regimes 2 and 3

In Regime 2, as stated before, the strains in the non-yielding  $x$ -reinforcement is assumed to be equal to  $\varepsilon_x \approx 0.8 f_{yx} / E_s$ , and  $\varepsilon_3 = -\varepsilon_{co}$  because the concrete crushes. The value of  $\cot^2 \theta$  for Regime 2 is given by  $\cot^2 \theta = (f_c - \rho_z f_{yz} + \sigma_z) / (\rho_z f_{yz} - \sigma_z)$ , equation (2.4b), and thus the value of  $\varepsilon_1$  will be



$$\varepsilon_1 = \varepsilon_x + (\varepsilon_x - \varepsilon_3) \cdot \left( \frac{f_c}{\rho_z f_{yz} - \sigma_z} - 1 \right) \quad (3.17)$$

Replacing equation (3.17) into the expression of  $f_c$ , one gets

$$\frac{30(\varepsilon_x - \varepsilon_3)}{\rho_z f_{yz} - \sigma_z} \cdot f_c^2 + (0.4 + 30\varepsilon_3) \cdot f_c - (f_c')^{2/3} = 0 \quad (3.18)$$

From the solution of the quadratic equation, equation (3.18), is possible to obtain

$$f_c = \frac{\rho_z f_{yz} - \sigma_z}{2 \cdot 30(\varepsilon_x - \varepsilon_3)} \left[ \sqrt{(0.4 + 30\varepsilon_3)^2 + 4 \cdot \frac{30(\varepsilon_x - \varepsilon_3)}{\rho_z f_{yz} - \sigma_z} \cdot (f_c')^{2/3}} - (0.4 + 30\varepsilon_3) \right] \quad (3.19)$$

Assuming the typical values for the strains,  $\varepsilon_x = 0.002$  and  $\varepsilon_{cw} = 0.002$ , one obtains

$$f_c^2 = \frac{25}{6} (\rho_z f_{yz} - \sigma_z) \cdot \left[ \sqrt{\frac{289}{2500} + \frac{12}{25} \cdot \frac{(f_c')^{2/3}}{\rho_z f_{yz} - \sigma_z}} - \frac{17}{50} \right] \quad (3.20)$$

for Regime 2, being the reinforcement in the  $x$ -direction stronger than that in the  $z$ -direction,  $(\rho_x f_{yx} - \sigma_x) > (\rho_z f_{yz} - \sigma_z)$ . In the case of  $(\rho_z f_{yz} - \sigma_z) > (\rho_x f_{yx} - \sigma_x)$ , which corresponds to Regime 3, the expression of  $f_c$  is given by

$$f_c^3 = \frac{25}{6} (\rho_x f_{yx} - \sigma_x) \cdot \left[ \sqrt{\frac{289}{2500} + \frac{12}{25} \cdot \frac{(f_c')^{2/3}}{\rho_x f_{yx} - \sigma_x}} - \frac{17}{50} \right] \quad (3.21)$$

## b.2) Regime 4

In Regime 4, the assumption of  $\varepsilon_x \approx 0.8 f_{yx} / E_s = 0.002$  results in  $\cot^2 \theta = 1$ , see equation (2.4d), and a constant value of  $\varepsilon_1$ ,



$$\varepsilon_1 = 0.002 + 0.004 \times 1 = 0.006 \quad (3.22)$$

Replacing the result of equation (3.22) into the expression of  $f_c$ , equation (3.12), one gets for Regime 4

$$f_c^4 = \frac{50}{29} (f_c')^{2/3} \quad (3.23)$$

Along the boundary between Regimes 2 and 4, see Figure 3.5, the weaker reinforcement in the  $z$ -direction is at onset of yielding,  $\sigma_{sz} = f_{yz}$ , and according to equilibrium conditions, equation (3.3b), and from equation (3.23), one obtains the condition:

From equilibrium conditions,

$$\rho_z \sigma_{sz} = \sigma_z + \tau_{xz} \tan \theta \quad \Rightarrow \quad \tau_{xz} = (\rho_z \sigma_{sz} - \sigma_z) \cdot \cot \theta \quad (3.24)$$

From the yield criterion for membrane elements in Regime 4, equation (2.1d)

$$\Phi_4 : \tau_{xz}^2 = f_c^2 / 4 \quad \therefore \quad \tau_{xz} = f_c / 2 \quad (3.25)$$

Associating equations (3.24) with (3.25) and replacing the value of  $f_c$ , which is given by equation (3.23), one gets

$$\frac{(f_c')^{2/3}}{(\rho_z f_{yz} - \sigma_z)} \cong 0.85 \quad (3.26)$$

along the boundary of Regimes 2 and 4.

### c) Design equations

Substituting the expressions for  $f_c$ , equations (20), (21), and (23), respectively, into the corresponding yield surface equations for membrane elements, equation (2.1), it is possible to obtain the following design expressions for the CMM

$$Y_1 : \tau_{xz}^2 = (\rho_x f_{yx} - \sigma_x) \cdot (\rho_z f_{yz} - \sigma_z) \quad (a)$$

$$Y_2 : \tau_{xz}^2 = (\rho_z f_{yz} - \sigma_z)^2 \cdot \left( \sqrt{2 + \frac{25}{3} \cdot \frac{(f_c')^{2/3}}{\rho_z f_{yz} - \sigma_z}} - \frac{29}{12} \right) \quad (b)$$

$$Y_3 : \tau_{xz}^2 = (\rho_x f_{yx} - \sigma_x)^2 \cdot \left( \sqrt{2 + \frac{25}{3} \cdot \frac{(f_c')^{2/3}}{\rho_x f_{yx} - \sigma_x}} - \frac{29}{12} \right) \quad (c) \quad (3.27)$$

$$Y_4 : \tau_{xz}^2 = \left[ \frac{25}{29} (f_c')^{2/3} \right]^2 \quad (d)$$

These expressions correctly represent the boundary of the ductile Regime 1 and yield conservative values of the ultimate strength for all failure regimes, allowing for safe and straightforward dimensioning.

Comparing the yield criteria developed by Nielsen (1971), equation (2.1), and the failure criteria given by equation (3.27), it is possible to draw the following conclusions: (i) for Regime 1 both equations are identical, and therefore the reinforcement design equations presented in Section 2.1 remain valid for equation (3.27a), but the condition of no-crushing of concrete is given by equation (3.16); (ii) for the other regimes, whose ultimate loads depend on  $f_c$ , the differences are based just on the way of evaluating  $f_c$ . For the failure criteria of the CMM, the response of concrete in compression is given by equation (3.12), which accounts for the compression softening of the concrete, resulting in a more realistic prediction of its behaviour.

If concrete crushes, therefore Regime 1 is no longer valid, but reinforcement design can still be carried out in regimes 2 or 3 if the concrete compressive stress does not surpass the effective concrete compressive strength in Regime 4, equation (3.23). However, the



designs equations for regimes 2 and 3 are nonlinear and the solution must be achieved by means of iterative numerical procedure. Rewriting equations (3.27b) and (3.27c), one gets

$$\begin{aligned} 23R_z^4 - 50(f_c')^{2/3}R_z^3 + 29\tau_{xz}^2R_z^2 + 6\tau_{xz}^4 &= 0 & (a) \\ 23R_x^4 - 50(f_c')^{2/3}R_x^3 + 29\tau_{xz}^2R_x^2 + 6\tau_{xz}^4 &= 0 & (b) \end{aligned} \quad (3.28)$$

where  $R_z = \rho_z f_{yz} - \sigma_z$ , Regime 2, and  $R_x = \rho_x f_{yx} - \sigma_x$  for Regime 3. As the values of  $R_z$  and  $R_x$  must be greater or equal to zero, the solution of equation (3.28) will thus be the first positive root found, whose value will correspond to the minimum reinforcement.

The reinforcement design cases covered by equation (3.28), which correspond to regimes 2 and 3, are interesting for reinforced membrane elements with moderate to high compressive stresses.

Below some numerical applications of the CMM design equations, equation (3.27), are shown. The first example (Regime 1), means that the formulation of Nielsen (1971) can be used and the second example (Regime 2) shows that the CMM formulation gives a 27 % increase of reinforcement with respect to Nielsen (1971) formulation.

a) Example 1

$$\begin{cases} \sigma_x = 1.60 \text{ MPa} \\ \sigma_y = -2.80 \text{ MPa} \\ \tau_{xz} = -1.10 \text{ MPa} \end{cases} \quad \begin{cases} h = 0.40 \text{ m} \\ f_{cd} = 16.70 \text{ MPa} \\ f_{ydx} = f_{ydz} = 435 \text{ MPa} \end{cases}$$

- Regime 1 - Case 3  $\begin{cases} \sigma_{sz} = 0 \\ \sigma_{sx} = 1.60 - \frac{(-1.10)^2}{-2.80} = 2.03 \text{ MPa} \end{cases}$

- Verification of concrete crushing:

Equation (2.7):  $\sigma_{c3} = 2.03 + 0 - 1.60 + 2.80 = 3.23 \text{ MPa}$

Equation (2.14):  $f_c^1 = \frac{(16.70)^{2/3}}{0.46 + 0.12 \cdot \frac{(2.03 - 1.60)}{[0 - (-2.80)]}} = 13.65 \text{ MPa}$





$$\sigma_{c3} < f_c^1 \Rightarrow OK!$$

- Calculation of reinforcement area:

$$\text{Equation (2.9): } \begin{cases} A_{sx} = \frac{2.03 \times 0.40}{435} = 1.87 \times 10^{-3} \text{ m}^2/\text{m} = 18.70 \text{ cm}^2/\text{m} \\ A_{sz} = 0 \end{cases}$$

b) Example 2

$$\begin{cases} \sigma_x = -4.80 \text{ MPa} \\ \sigma_y = 0.20 \text{ MPa} \\ \tau_{xz} = -0.70 \text{ MPa} \end{cases} \quad \begin{cases} h = 0.40 \text{ m} \\ f_{cd} = 16.70 \text{ MPa} \\ f_{ydx} = f_{ydz} = 435 \text{ MPa} \end{cases}$$

- Regime 1 - Case 2  $\begin{cases} \sigma_{sx} = 0 \\ \sigma_{sz} = 0.20 - \frac{(-0.70)^2}{-4.80} = 0.30 \text{ MPa} \end{cases}$

- Verification of concrete crushing in Regime 1:

$$\text{Equation (2.7): } \sigma_{c3} = 0 + 0.30 - (-4.80) - 0.20 = 4.90 \text{ MPa}$$

$$\text{Equation (2.14): } f_c^1 = \frac{(16.70)^{2/3}}{0.46 + 0.12 \cdot \frac{[0 - (-4.80)]}{(0.30 - 0.20)}} = 1.05 \text{ MPa}$$

$$\sigma_{c3} > f_c^1 \Rightarrow \text{Not OK!}$$

- Verification of the possibility of reinforcement design in Regime 2

$$\text{Equation (3.23): } f_c^4 = \frac{50}{29} (16.70)^{2/3} = 11.26 \text{ MPa}$$

$$\sigma_{c3} < f_c^4 \Rightarrow OK!$$

From equation (3.28b),

$$23 \cdot R_z^4 - 50 \times (16.70)^{2/3} R_z^3 + 29 \times (-0.70)^2 R_z^2 + 6 \times (-0.70)^4 = 0$$



$$23 \cdot R_z^4 - 326.67R_z^3 + 14.21R_z^2 + 1.44 = 0$$

The solution of the equation gives, as a valid value:  $R_z = 0.18 \text{ MPa}$

$$R_z = \sigma_{sz} - \sigma_z \Rightarrow \sigma_{sz} = R_z + \sigma_z$$

$$\sigma_{sz} = 0.18 + 0.30 = 0.38 \text{ MPa}$$

- Calculation of reinforcement area:

$$\text{Equation (2.9): } \begin{cases} A_{sx} = 0 \\ A_{sz} = \frac{0.38 \times 0.40}{435} = 0.35 \times 10^{-3} \text{ m}^2/\text{m} = 3.50 \text{ cm}^2/\text{m} \end{cases}$$

*The reinforcement area for this case according to Nielsen (1971) formulation is  $(0.30 \times 0.40 / 435) = 2.76 \text{ cm}^2 / \text{m}$ . Thus, the increase of reinforcement when using the CMM formulation is about 27%.*

## 4 Numerical Implementation

This Chapter presents the computer program and the numerical routines developed to implement the reinforcement designs equations for orthogonally reinforced, cracked membrane elements, described in the previous Chapter.

Figure 4.1 illustrates the input data window of the computer program, which executes the numerical routines, according to the flowchart described in Section 4.1.

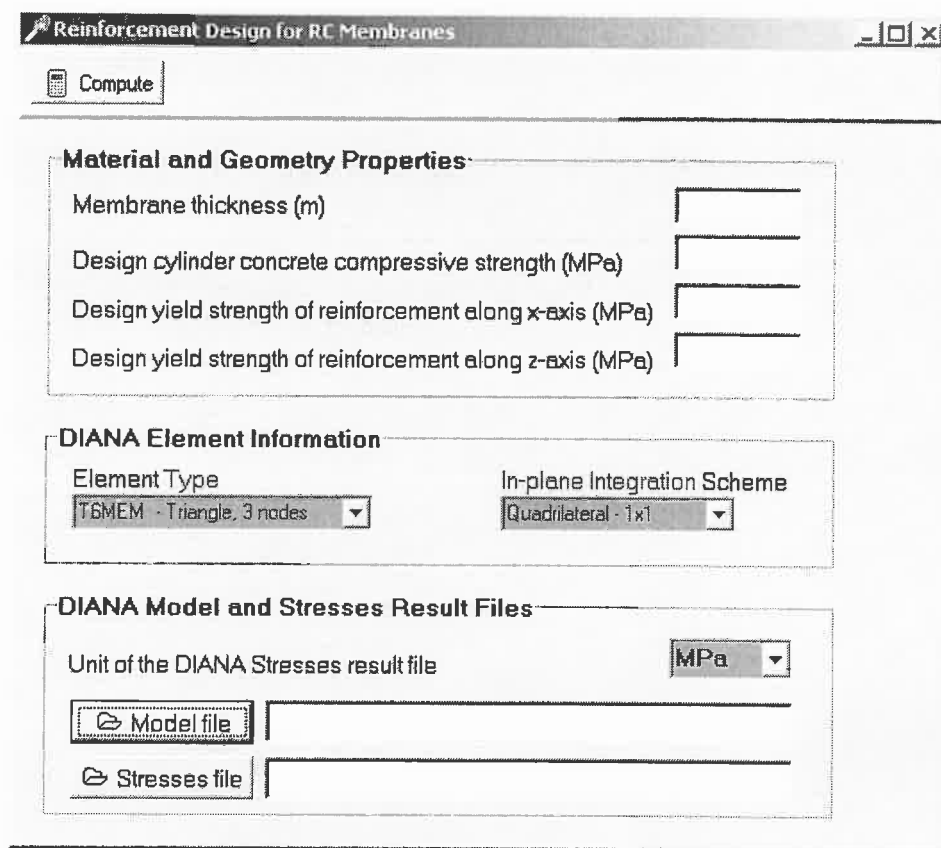


Figure 4.1 – Input data window of the computer program

It can be seen that the input data for the reinforcement design computations is rather simple. In the “Material and Geometry Properties” box, the user inputs the thickness and material properties of the structure. The two other boxes deal with the data provided by DIANA<sup>®</sup> 8.1 finite-element analysis program. In “DIANA Element Information” box, the user selects the finite-element type and integration scheme which were used for the elastic

analysis of the structure in DIANA. Finally, in “DIANA model and Stresses Result Files” the user loads the files of the model and stresses result by clicking on buttons “model file” and “stresses file”. The files of the model and stresses result are text files containing respectively the data of the structure modeled in finite elements for DIANA and the result of stresses obtained from the linear elastic analysis performed in DIANA for the structure.

With the input data completed, the user can process the data by clicking on “Compute” button. Then the following window will be displayed, Figure 4.2, where one can find the reinforcement area results which have been calculated. Besides, the program generates an output file with the results for post-processing in DIANA, which can be loaded through the graphical user interface of DIANA.

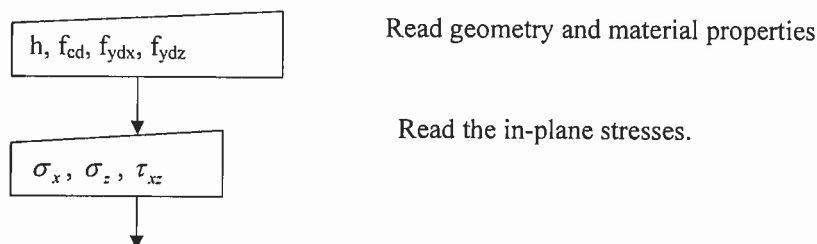
Elm	Node	Asx (cm <sup>2</sup> /m)	Asz (cm <sup>2</sup> /m)	Tc3 (MPa)	Regime
1	1	0.00000E+00	0.00000E+00	0.80700E+01	1
1	10	0.00000E+00	0.00000E+00	0.62160E+01	1
1	2	0.00000E+00	0.00000E+00	0.43630E+01	1
1	13	0.47939E+01	0.00000E+00	0.45538E+01	1
1	5	0.14406E+02	0.00000E+00	0.52677E+01	1
1	15	0.91171E+01	0.00000E+00	0.42068E+01	1
1	4	0.52331E+01	0.00000E+00	0.32904E+01	3
1	12	0.00000E+00	0.00000E+00	0.53985E+01	1
2	2	0.00000E+00	0.00000E+00	0.47841E+01	1
2	11	0.00000E+00	0.00000E+00	0.39442E+01	1
2	3	0.00000E+00	0.00000E+00	0.31053E+01	1

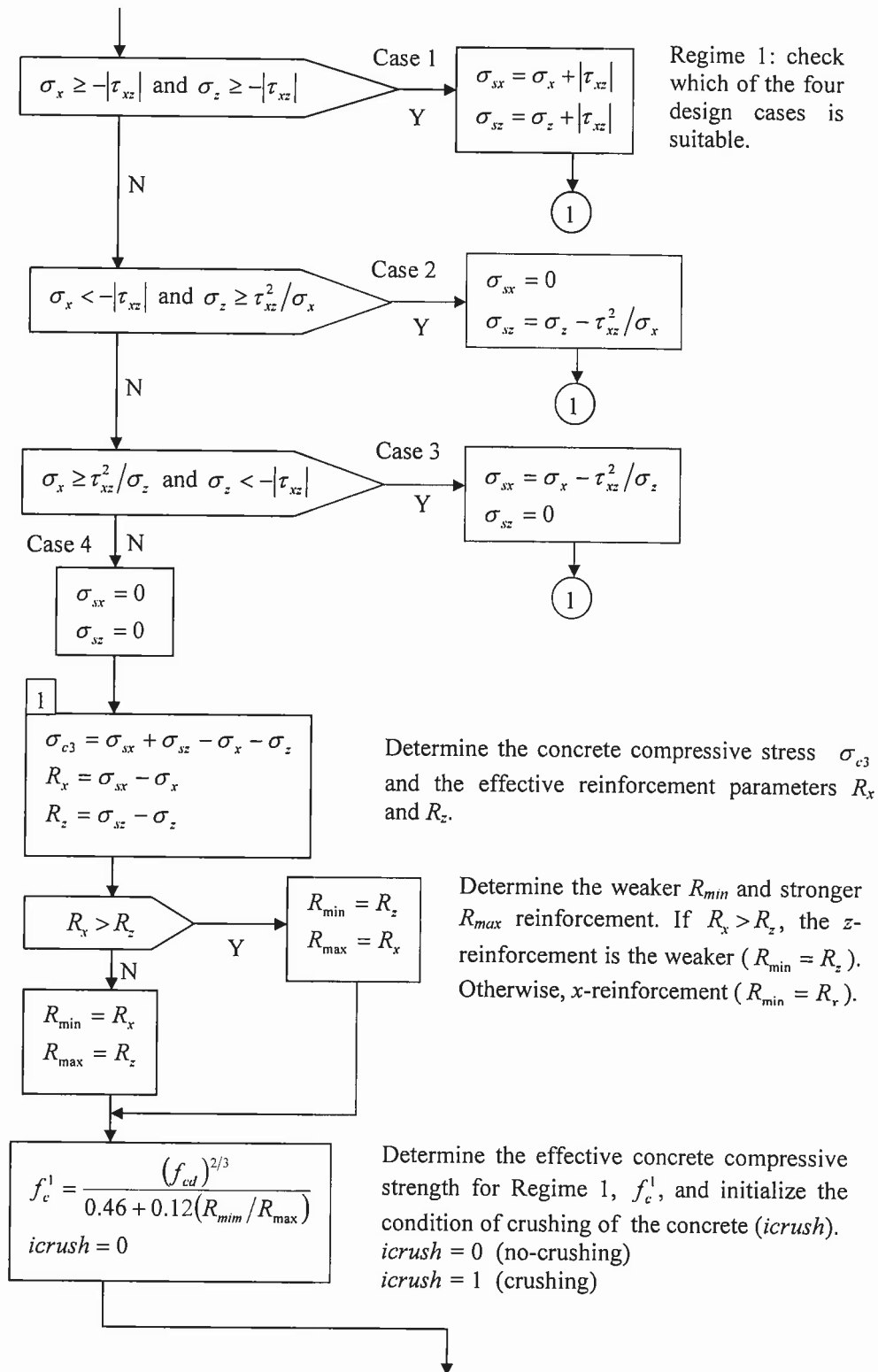
Figure 4.2 – Window of the reinforcement area results ( $Tc3 = \sigma_{c3}$ )

#### 4.1 Numerical Routines

The flowchart below presents the numerical routines which have been used to implement the reinforcement design equations.

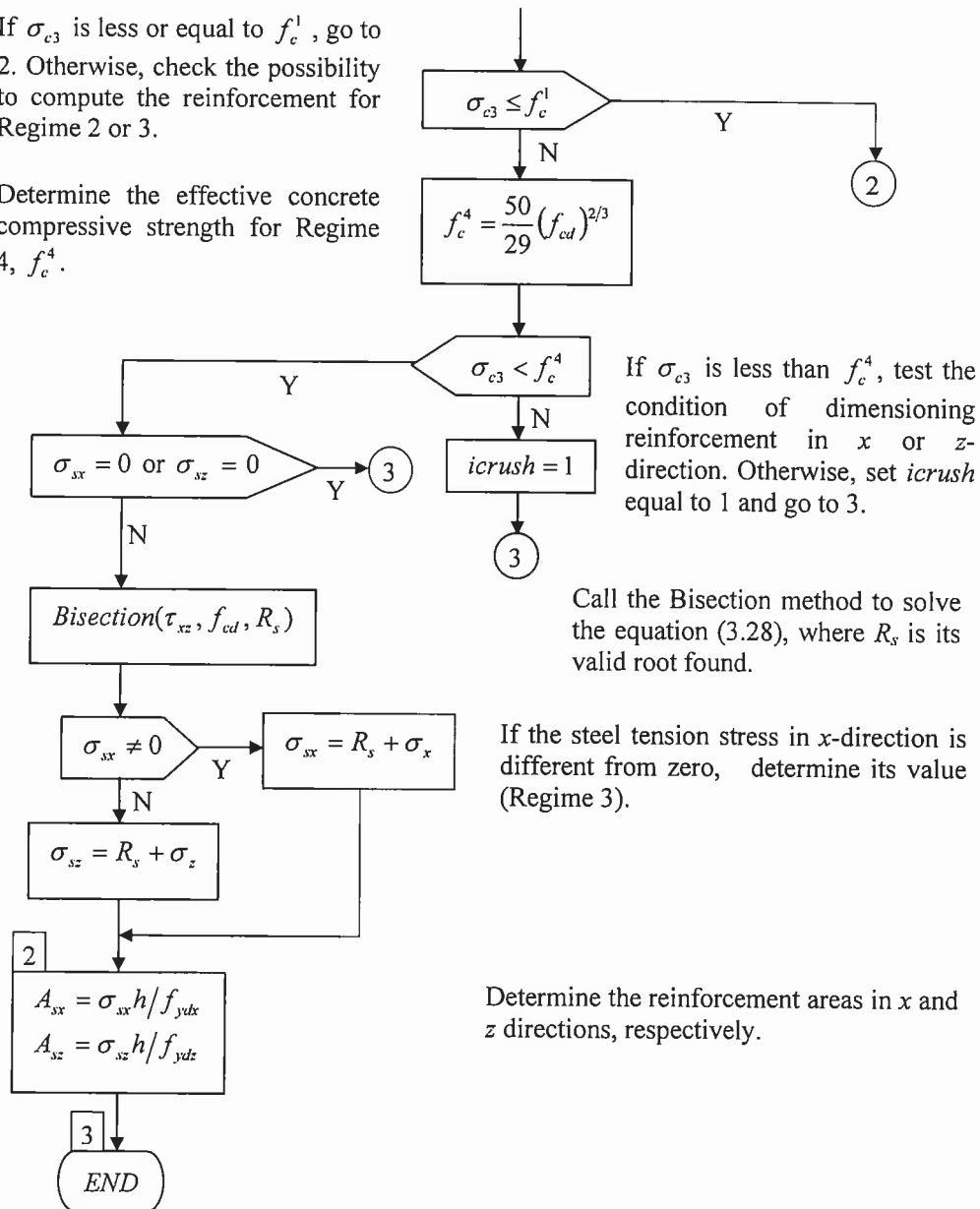
a) *CMM*membrane routine





If  $\sigma_{c3}$  is less or equal to  $f_c^1$ , go to 2. Otherwise, check the possibility to compute the reinforcement for Regime 2 or 3.

Determine the effective concrete compressive strength for Regime 4,  $f_c^4$ .



If  $\sigma_{c3}$  is less than  $f_c^4$ , test the condition of dimensioning reinforcement in  $x$  or  $z$ -direction. Otherwise, set  $icrush$  equal to 1 and go to 3.

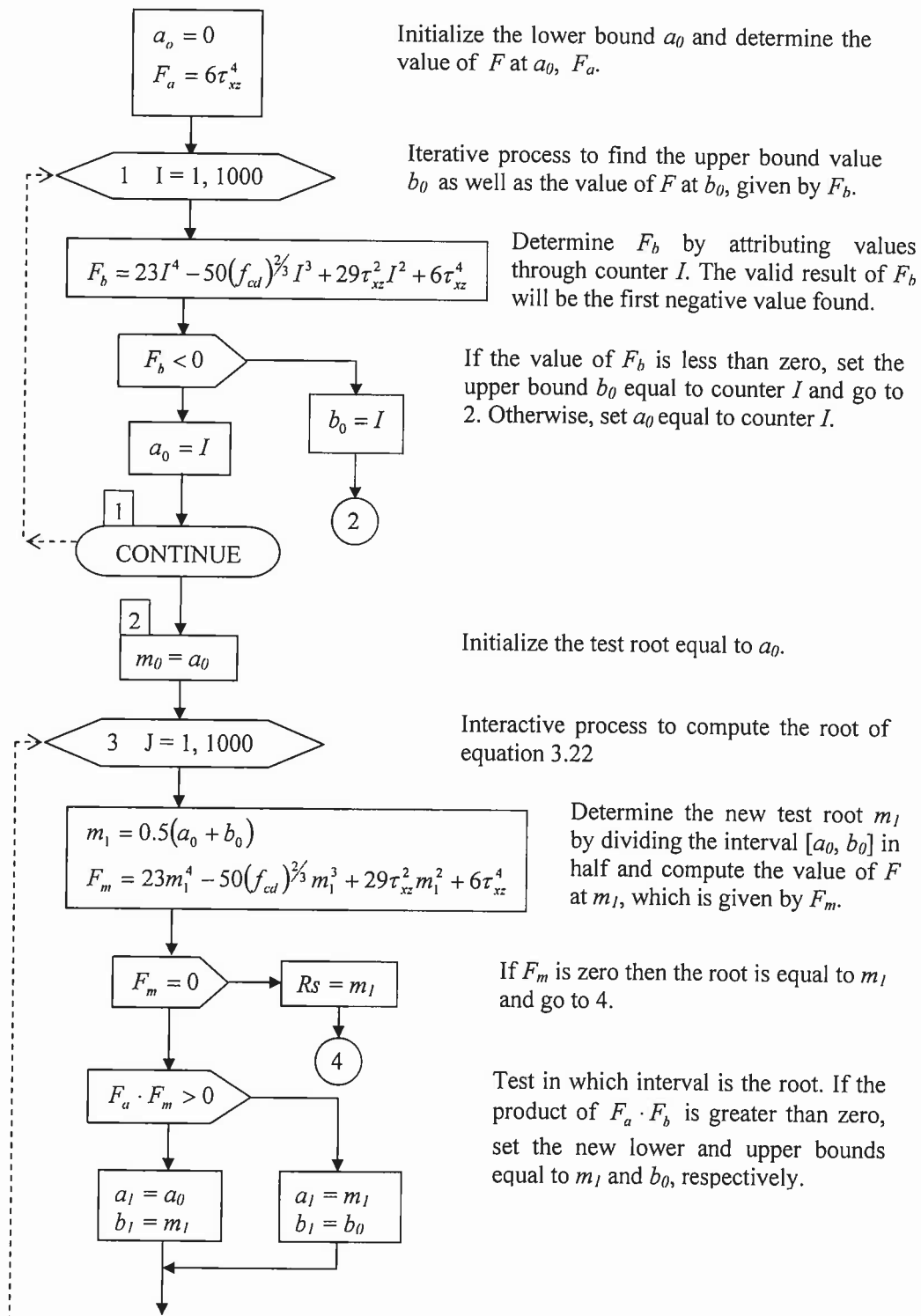
Call the Bisection method to solve the equation (3.28), where  $R_y$  is its valid root found.

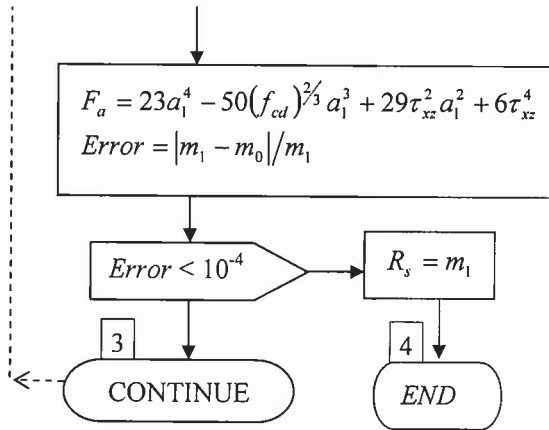
If the steel tension stress in  $x$ -direction is different from zero, determine its value (Regime 3).

Determine the reinforcement areas in  $x$  and  $z$  directions, respectively.

### b) Bisection Routine

This routine finds the solution of equation (3.22) through the method of bisection. Setting equation (3.28) as  $F(x) = 23x^4 - 50(f_{cd})^{2/3}x^3 + 29\tau_{xz}^2x^2 + 6\tau_{xz}^4$ , where  $x \in \mathfrak{R}$ , the steps below were implemented to find the root  $R_y$ .





Determine  $F_a$  at  $a_1$  and compute the error for the approximation.

If *Error* is less than 0.0001, set the root of equation (3.28) equal to  $m_1$  and go to 4.



## 5 Application Examples

This Section will presents two application examples of deep beams using the computer program developed for the reinforcement design of cracked, orthogonally concrete elements subjected to in-plane forces. The results obtained this way will then be compared to those calculated according to the traditional formulation, Nielsen (1971).

The elastic analyses, as mentioned before, were all performed in DIANA<sup>®</sup> 8.1 finite element program. The results of reinforcement areas computed by the computer program are stored in output files in text format and also in DIANA output format for post-processing in its graphical interface.

### 5.1 Deep Beam With One Opening

The concrete deep beam shown in Figure 5.1 was analyzed by Schlaich (1987). It is a simply supported structure with an opening on the left side, carrying a point load of 3000 kN on top.

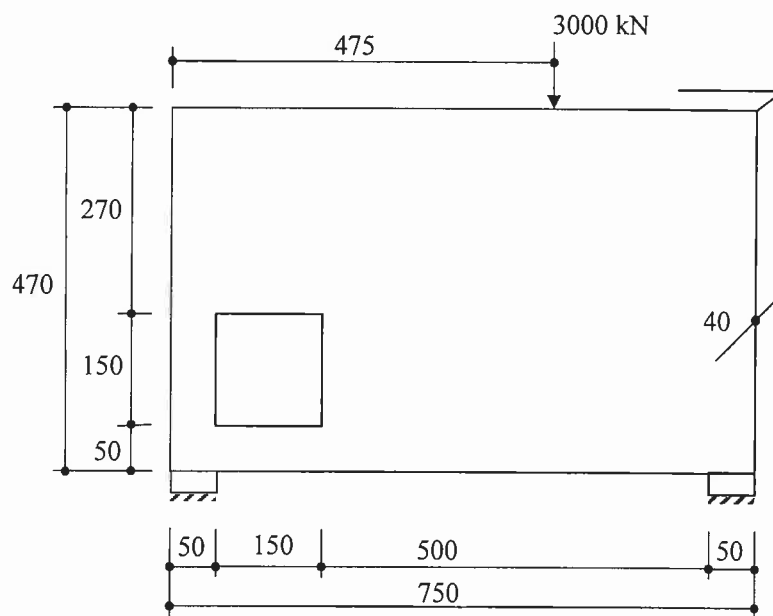


Figure 5.1 – Geometry of the deep beam with one opening (dimensions in centimeters)

For the linear-elastic FEM analysis, the structure was modeled using eight-node quadrilateral plane stress elements with two by two in-plane Gauss integration. The material properties (concrete) used were 30.5 MPa and 0.2, for Young's modulus and Poisson ratio, respectively. Figure 5.2 shows the stress results for the elastic analysis of the deep beam.

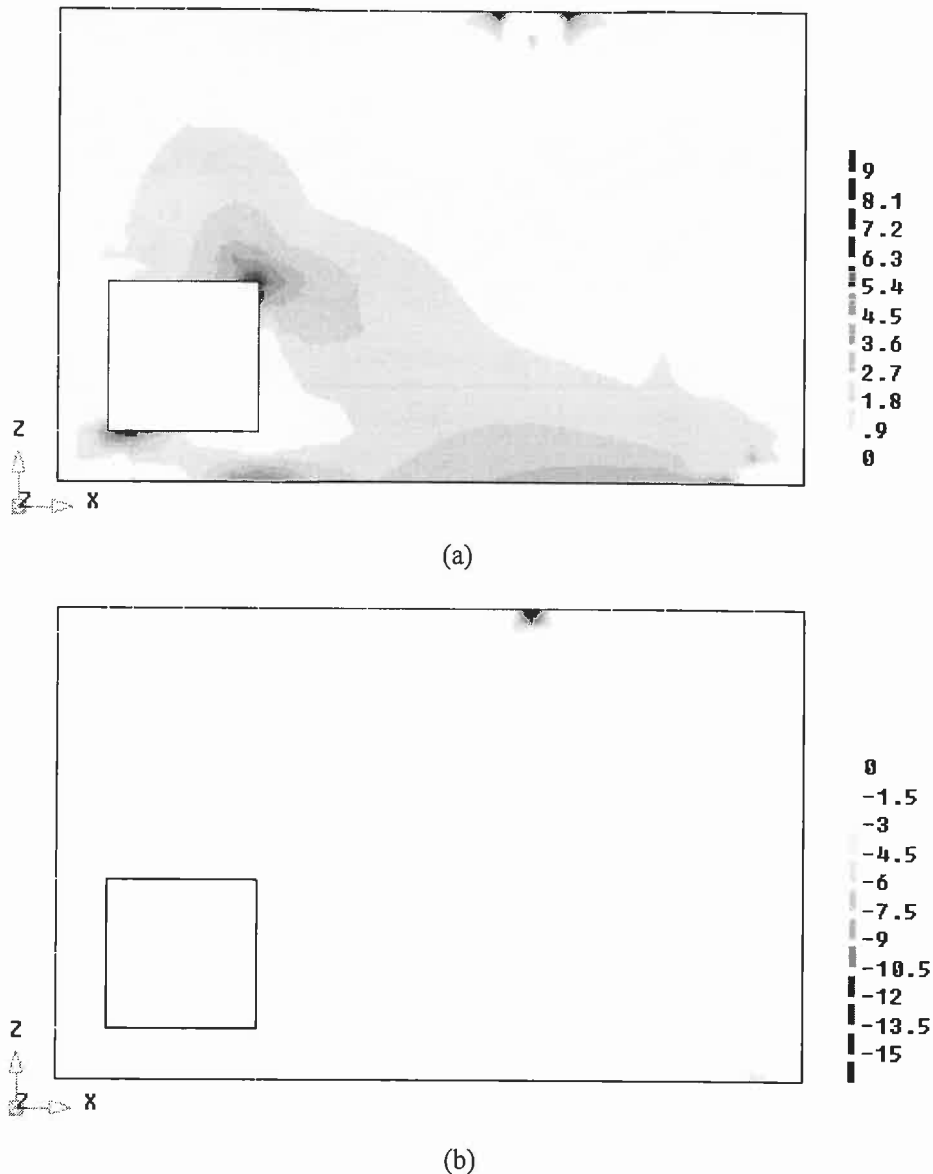


Figure 5.2 –Principal stress results (in MPa): a)  $\sigma_1$ ; b)  $\sigma_3$

As one can observe in Figure 5.2, due to the opening, the distribution of stress undergoes considerable changes in comparison to the usual distribution of stress in deep beams, thus preventing the formation of a unique compression field stress, which could connect the applied load to the left support.

For the reinforcement design in both formulations, a design compressive strength of concrete  $f_{cd} = 16.67$  MPa and a design yield strength of reinforcement in both directions  $f_{yx} = f_{yz} = 435$  MPa, were considered.

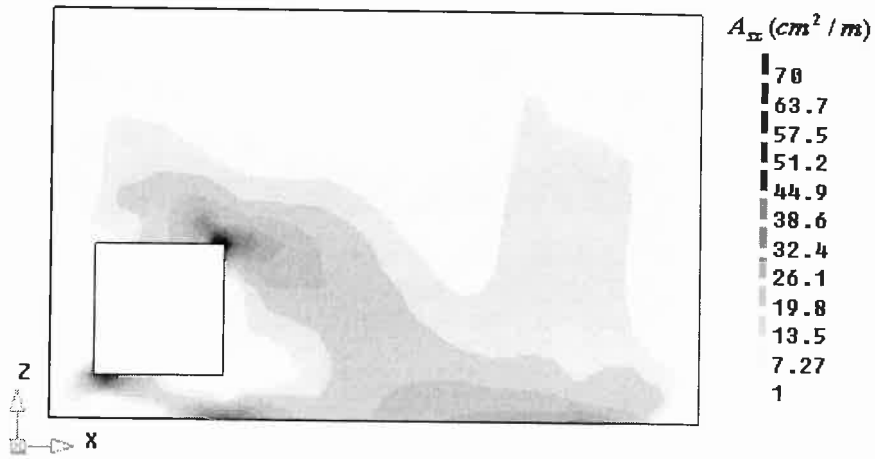
Finally, Figure 5.3 and Figure 5.4 show the graphical representation of reinforcement distribution in  $x$  and  $z$  directions calculated according to the traditional and CMM formulations.

As one can see, according to Figure 5.3 and Figure 5.4 the graphical distributions of reinforcement for the CMM and traditional formulations are very similar. This fact happens because just 19% of the integration points had stress state that fell into regimes 2 and 3, which strictly refer to the CMM formulation, resulting thus in little increase in the total amount of reinforcement. Nevertheless, locally large variation can be found (more than 100% or 3 cm<sup>2</sup>/m), see Figure 5.5(a,b). In absolute terms, the largest variations occur at the right support and the small vertical pier around the left opening. The additional reinforcement areas provided by carrying out the design in regimes 2 and 3 are shown in Table 5.1. The total difference is only about 0.6%.

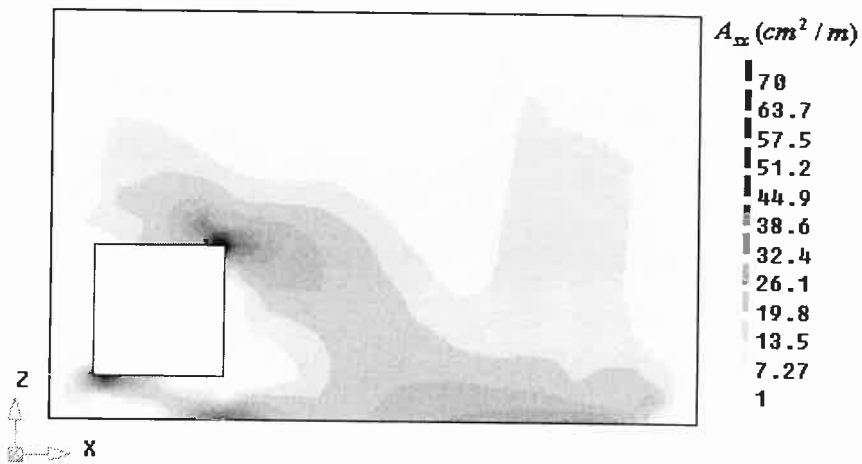
Table 5.1 – Comparison: total reinforcement areas

Formulation	$A_{sx}$ (cm <sup>2</sup> /m)	$A_{sz}$ (cm <sup>2</sup> /m)	$A_{stot}$ (cm <sup>2</sup> /m)
Traditional	4875.49	5205.31	10080.80
CMM	4920.75	5216.75	10137.50
Differences	45.26	11.44	56.70

With reference to the verification of the crushing of concrete, there are also differences. From the traditional formulation six integration points crushed in the concrete whereas in the CMM ten integration points were pointed out, see Figure 5.5(c,d). The reason for that is due to the distinct treatment of crushing of the concrete for the formulations, as described in Sections 2.1 and 3.2.

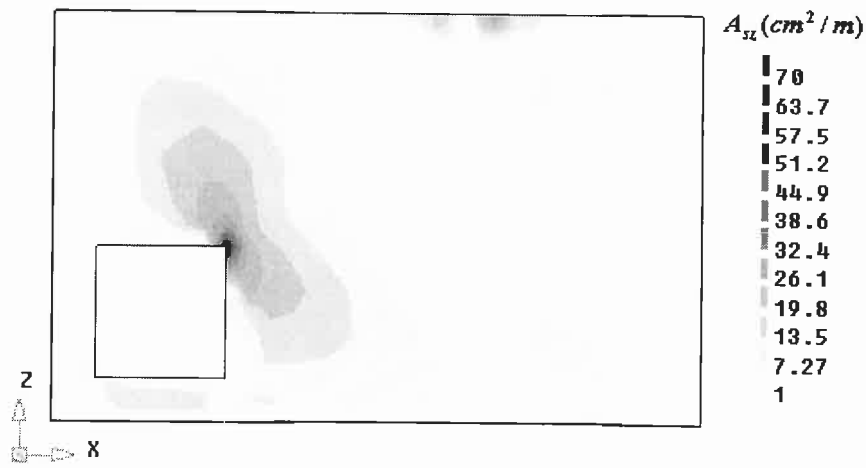


(a)



(b)

Figure 5.3 – Reinforcement areas in  $x$ -direction for formulations: a) Traditional; b) CMM.



(a)



(b)

Figure 5.4- Reinforcement areas in z-direction for formulations: a) Traditional;  
b) CMM

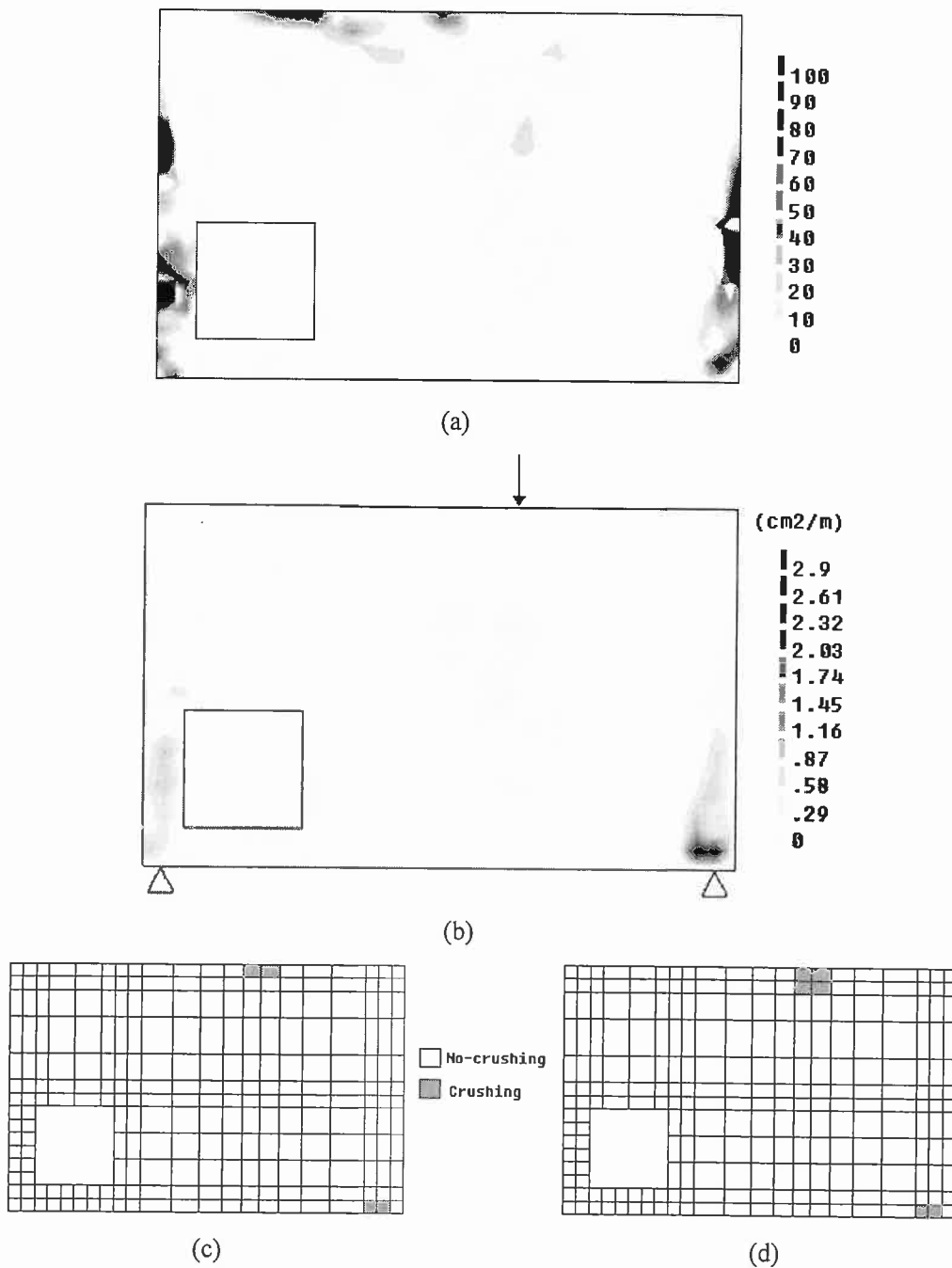


Figure 5.5 – Differences between the traditional and CMM formulations: a) additional total reinforcement area yielded by the CMM, in a) percentage and b) absolute value; Concrete crushing according to the formulations c) traditional and d) CMM.

## 5.2 Deep Beam With Two Openings

The second deep beam, shown in Figure 5.6, was analyzed by Oliveira *et al* (1998). It is also a simply supported structure with two openings, carrying a load of 20 kN/cm on top, located at mid-span and distributed in a length of 30 cm.

To perform the linear-elastic FEM analysis, the structure was modeled with the same plane stress elements and integration scheme used in the first application example. The material properties adopted for the concrete were those given by Oliveira (1998), i.e. 34 MPa and 0.2, for the Young's modulus and the Poisson's ratio, respectively. Figure 5.7 shows the principal stress results for the elastic analysis of the deep beam with two openings.

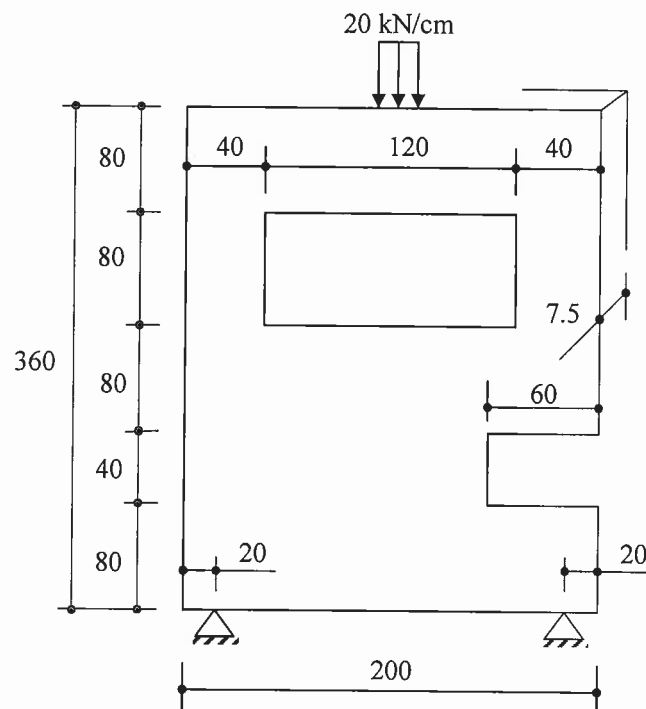


Figure 5.6 – Geometry of deep beam with two openings (dimensions in centimeters)

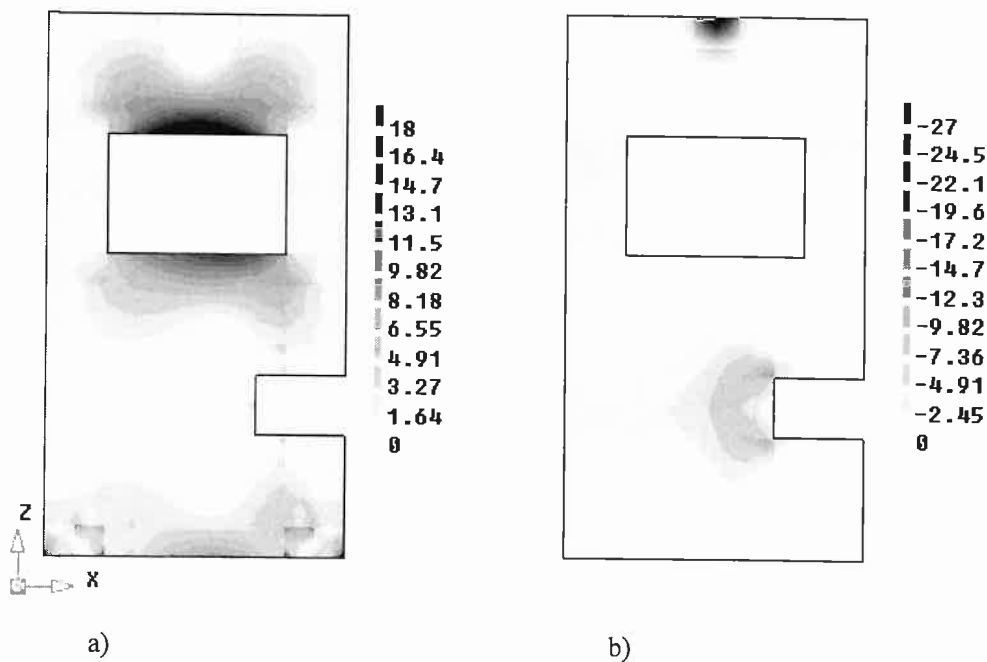


Figure 5.7 - Principal stress results (in MPa): a)  $\sigma_1$ ; b)  $\sigma_3$

From Figure 5.7a one can see the distribution of tensile stresses in the deep beam, which is mostly responsible for the distribution of reinforcement in the structure. The behavior of the structure is heavily controlled by the top opening and also by the asymmetrical position of the bottom opening.

For the reinforcement design in both formulations, the values specified by Oliveira *et al* (1998) were again adopted, i.e. a design compressive strength of concrete  $f_{cd} = 34$  MPa and a design yield strength of reinforcement in both directions  $f_{yk} = f_{yk} = 444$  MPa .

Figure 5.8 and Figure 5.9 show the graphical representation of reinforcement distribution in both directions, calculated according to the traditional and CMM formulations.



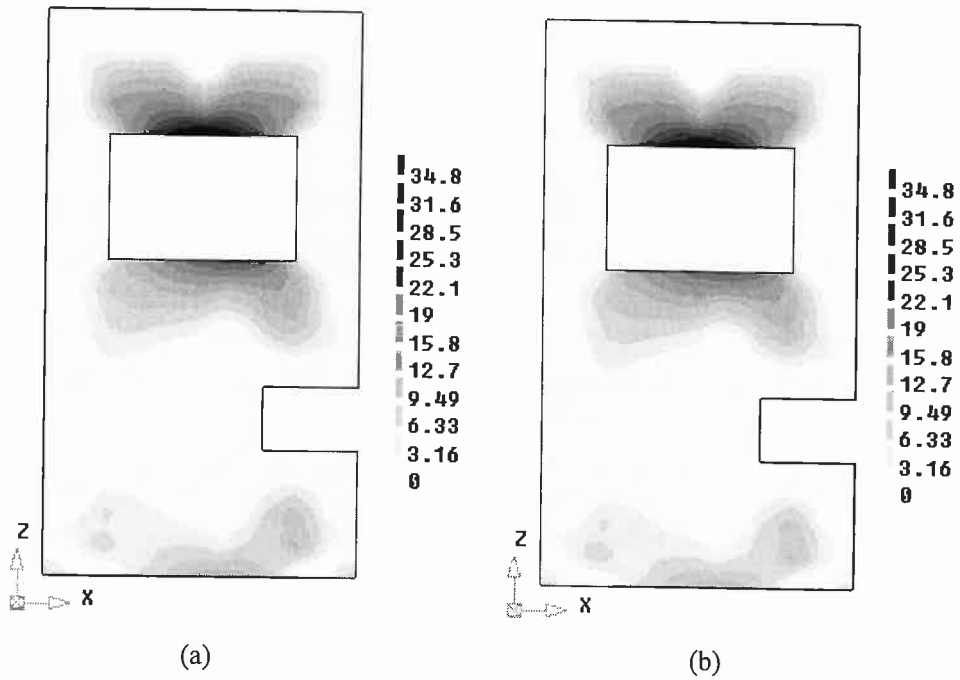


Figure 5.8 - Reinforcement areas in  $x$ -direction for formulations: a) Traditional;  
b) CMM

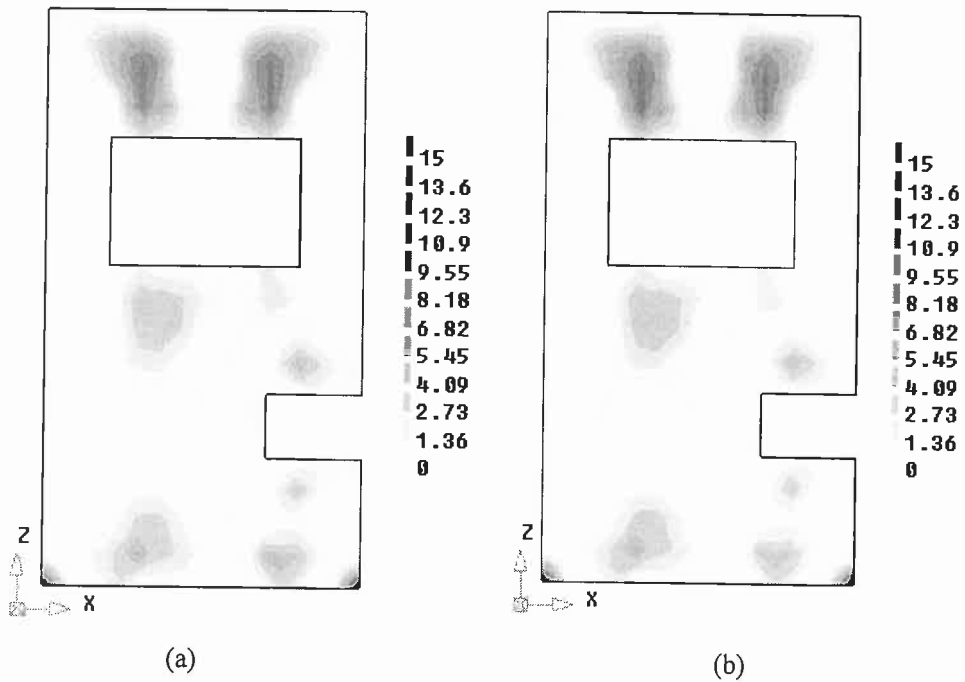


Figure 5.9 - Reinforcement areas in  $z$ -direction for formulations: a) Traditional;  
b) CMM

As in the first application, the graphical distributions of reinforcement for the CMM and traditional formulations are again very similar, see Figure 5.8 and Figure 5.9. In this example just 15% of the integration points had stress state that fell into regimes 2 and 3 (CMM formulation), resulting in even less increase in the total amount of reinforcement. In this case, the variation in reinforcement is rather low (only up to 1 cm<sup>2</sup>), see Figure 5.10(a,b). The additional reinforcement areas provided by carrying out the design in Regimes 2 and 3 are shown in Table 5.2. The total difference is similar to the previous example, about 0.5%.

Table 5.2- Comparison: total reinforcement areas

Formulation	$A_{sx}$ (cm <sup>2</sup> /m)	$A_{sz}$ (cm <sup>2</sup> /m)	$A_{stot}$ (cm <sup>2</sup> /m)
Traditional	3237.72	698.33	3936.05
CMM	3251.98	704.78	3956.76
Differences	14.26	6.45	20.71

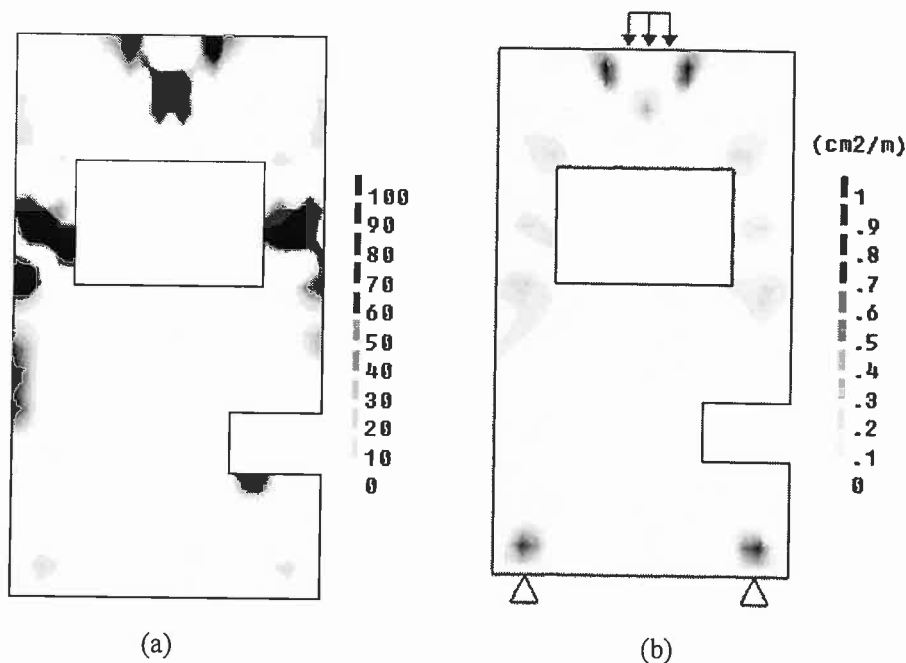


Figure 5.10 – Additional total reinforcement area yielded by the CMM, in a) percentage and b) absolute value.

For the verification of concrete crushing, the differences between the traditional and CMM formulations are more significant than the distributions of reinforcement, having the traditional formulation pointed out only 4 integration points for the concrete crushing, while the CMM formulation pointed out 46, see Figure 5.11.

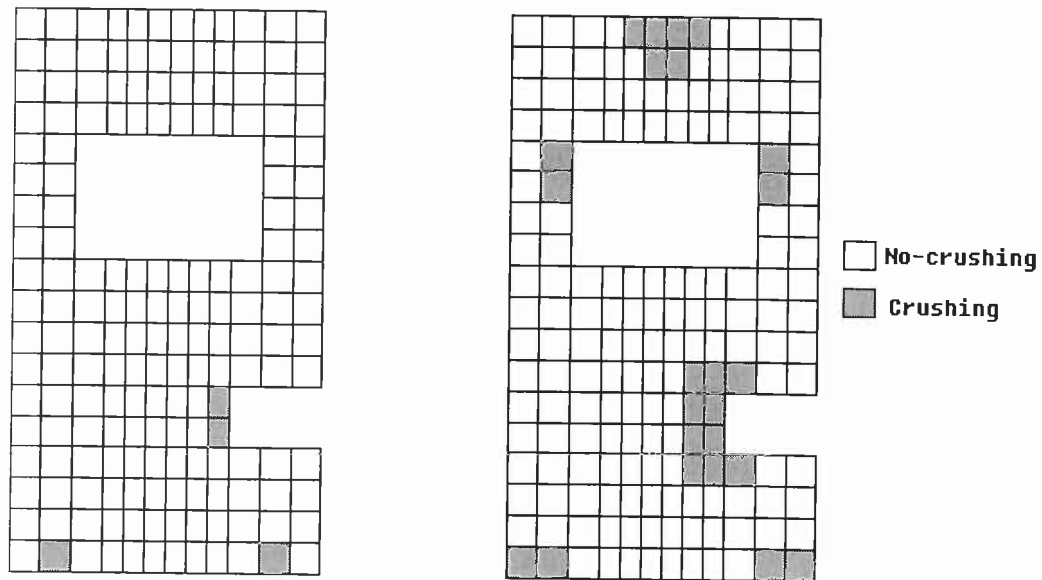


Figure 5.11 - Concrete crushing according to the formulations: b) traditional; c) CMM.



## 6 Conclusions

This report presents the implementation of design equations for orthogonally reinforced, cracked membrane elements, which were derived by Kaufmann (2002) from his theoretical analysis model for the cracked behavior of RC membrane elements. The results obtained through the CMM formulation for the application example showed just a minor increase in the total amount of reinforcement when compared to those obtained from the traditional formulation, Nielsen (1971). Nevertheless, in a few integration points rather significant changes could be found. Because the design equations from CMM yield a more realistic response of concrete at ultimate state, the results of reinforcement areas increase when concrete crushes, regimes 2 and 3. Besides, the condition of concrete failure by crushing is more severe than the traditional formulation.

In conclusion, the application of design equations of the CMM formulation for practical design purposes seems to be of some relevance as the traditional formulation can give unsafe results. Besides, recent investigations show that the ultimate loads predicted by these design equations have good correlation with experimental results, Kaufmann (2002) and Carbone *et al* (2001). Therefore, it is recommended that the novel, more comprehensive and still straightforward formulation is adopted for design purposes.



## 7 References

CARBONE, V.I., GIORDANO, L., MANCINI, G., (2001) - Design of RC membrane elements, *Structural Concrete*, 2001(4), p. 213-223 (2001)

CEB-FIP (1991) - Model Code, Final Draft, Bulletin d'Information n<sup>os</sup> 203, 204 and 205.

KAUFMANN, W. (2002) - Analysis and design of structural concrete elements subjected to in-plane forces, *Structural Concrete*, 2002(3), p. 155-158.

KAUFMANN, W., MARTI, P. (1998) - Structural concrete: cracked membrane model, *J. Struc. Engrg., ASCE*, 124 (12), p. 1467-1475.

LOURENÇO, P.B.; FIGUEIRAS, J.A. (1995) - A solution for the design of reinforced concrete plates and shells, *J. Struc. Engrg., ASCE*, 121(5), p. 815-823.

LOURENÇO, P.B.; FIGUEIRAS, J.A. (1993) - Automatic design of reinforcement in concrete plates and shells, *Engineering Computations*, 10 (6), p. 519-541.

MARTI, P.; ALVAREZ, M.; KAUFMANN, W.; SIGRIST, V. (1998) – Tension Chord Model for Structural Concrete, *Structural Engineering, IABSE*, 8, No. 4, p. 287-298.

NIELSEN, M.P. (1964) - Yield conditions for reinforced concrete shells in the membrane state, *Non-classical shell problems*, North-Holland, Amsterdam, p. 1030-1040.

NIELSEN, M.P. (1971) – On the strength of reinforced concrete disks, *Acta Polytechnica Scandinavica, Civ. Engrg. Constr. Service*, Copenhagen, Denmark.

OLIVEIRA, L.P.; BASTOS, A.M.S.T.; FIGUEIRAS, J.A. (1998) – Behavior at failure of reinforced concrete wall elements (in Portuguese), In: *Jornadas Portuguesas de Engenharia de Estruturas, LNEC, Lisboa, Portugal, 25-28 Nov.*, p. 431-440.

VECCHIO, F.J., COLLINS, M.P. (1986) - The modified compression field theory for reinforced concrete elements subjected to shear, *ACI Journal*, 83(2), p. 219-231.